FCTUC FACULDADE DE CIÊNCIAS E TECNOLOGIA
UNIVERSIDADE DE COIMBRA

Gilberto Miguel Ribeiro Silva

# Time-frequency and coherence based studies of the neural correlates of visual perception

*Dissertação apresentada à Universidade de Coimbra para cumprimento dos requisitos necessários à obtenção do grau de Mestre em Engenharia Biomédica*

Supervisor:

M.D., Ph.D. Miguel Castelo-Branco

Coimbra, 2014

Este trabalho foi desenvolvido em colaboração com:

ICNAS – Instituto de Ciências Nucleares Aplicadas à Saúde

IBILI – Institute for Biomedical Imaging and Life Sciences

Faculdade de Ciências e Tecnologias da Universidade de Coimbra

*Aos meus avós*

*Pedro e José,*

# Agradecimentos

Este trabalho não seria o mesmo se não tivesse uma participação, mesmo que simples, de todos os que me rodeiam e que fizeram parte do meu dia-a-dia ao longo de toda a minha formação.

Agradeço ao Professor Doutor Miguel Morgado, pelo seu constante acompanhamento e preocupação com o bem-estar dos estudantes do Mestrado Integrado em Engenharia Biomédica.

Ao Professor Doutor Miguel Castelo-Branco, pela supervisão, orientação, por todo o suporte e motivações; por conseguir condições estruturais e financeiras para receber estudantes e investigadores; por ser uma referência como professor, como investigador e como pessoa.

Ao Doutor Gabriel Costa, Doutora Inês Violante e João Castelhano pela disponibilidade e incansável ajuda na resolução dos problemas que surgiram, nas sugestões que deram e pelo acompanhamento ao longo de todo este último ano. Por todo o valor que acrescentaram a este trabalho. Agradeço ainda à Doutora Inês Violante e à Doutora Maria Ribeiro pela cedência dos dados de elecroencefalografia, imprescindíveis no desenvolvimento desta tese.

Aos meus amigos, pelo companheirismo e pela presença indispensável.

Aos meus pais, pelo suporte, confiança e esforço. Agradeço especialmente aos meus irmãos, Anabela e Pedro, e pela constante motivação que muitas vezes foi necessária.

À Tânia, pela terna amizade, dedicação, compreensão e ajuda.

A todos vós, obrigado.

*There is no such thing as a disembodied mind.*
*The mind is implanted in the brain, and*
*the brain is implanted in the body*
*António Damásio*

# Abstract

Over the recent years, neurosciences' field has been focused in understanding the complexity of the human brain, through the application of a myriad of techniques, which act as "windows" in the exploration of the more complex and less known human organ.

Exploring the strong advantage of the electroencephalogram and its powerful temporal resolution, the aim of this thesis is to expand knowledge and build methods of analyzing brain oscillations, including the study of their features in time and frequency.

Presently, numerous references are made to the current relationship between oscillations and perception, attention, memory, learning, information integration among others, providing a growing enthusiasm in the application of oscillations to unravel the physiological mechanisms involved in these processes.

However, the classification of oscillations in humans involves quite complex approaches and is a controversial topic in neuroscience. This complexity is caused, in one hand, by the difficulty in relating the mechanisms at the basis of formation of such oscillations, where the origin is not clear: biological sources and mechanisms which contribute to their formation. On the other hand, dissimilar hints of the information that apparently relates to this issue like genetics or inter-individual variability. Nevertheless, a principle seems certain: the stability of the oscillations at the individual level.

In this thesis, respecting an automated and independent analysis will be treated and implemented methods of pre-processing and analysis "data-driven" to the identification of bands in any kind of "time-frequency" spectra. With application of created algorithms, will be searched any relation between bands of oscillations (power and phase synchrony analysis) between groups (control and individuals with neurofibromatosis type-1) and between BOLD signals and the GABA levels.

# Resumo

Ao longo dos últimos anos, o estudo na área das neurociências tem vindo a focar-se na compreensão da complexidade do cérebro humano; utilizando as mais variadas técnicas que, evoluindo ao longo do tempo, se transformam em potenciais "janelas" na exploração do mais complexo e menos conhecido órgão humano.

Explorando a forte vantagem do electroencefalograma e a sua poderosa resolução temporal, o objectivo desta tese é aprofundar conhecimentos e construir métodos de análise das oscilações cerebrais, nomeadamente, o estudo das suas características em tempo e frequência.

Actualmente são realizadas inúmeras referências à relação entre as oscilações e percepção, atenção, memória, aprendizagem, integração de informação, entre outras. A compreensão destes mecanismos pode ser inferida através das oscilações, pelo que existe uma crescente vontade em fazer uso da interpretação das mesmas para conhecimento dos diversos mecanismos cognitivos inerentes.

No entanto, a classificação das oscilações em humanos é um tema complexo, e que carece de consenso no seio da comunidade científica. Por um lado, surge a dificuldade de relacionar os mecanismos na base da formação de tais oscilações, não sendo claras as fontes biológicas que contribuem para a sua formação. Por outro, temos as nuances na informação que, aparentemente, se relacionam com esta questão (sejam características genéticas ou até variabilidade inter-individual). No entanto, um princípio parece certo: a estabilidade das oscilações a nível individual.

Nesta tese, valorizando uma análise automatizada e independente, serão abordados e implementados métodos de pré-processamento e análise "data-driven" para identificação de bandas em qualquer tipo de imagem "time-frequency". Aplicando os algoritmos criados, será procurada relação entre bandas de oscilações entre grupos (controlo e indivíduos com neurofibromatose tipo-1) e entre sinais hemodinâmicos de BOLD e níveis de GABA.

*(Este documento não se encontra ao abrigo do novo acordo ortográfico)*

# Abbreviations

- *AP – Action Potential*
- *BCI – Brain Computer Interface*
- *BOLD - Blood Oxygenation Level Dependent*
- *CNS – Central Nervous system*
- *DFT – Discrete Fourier Transform*
- *ECoG – Electrocorticography*
- *EEG – Electroencephalogram*
- *EPSP – Excitatory Postsynaptic Potential*
- *ERD – Event Related Desynchronization*
- *ERPCOH – Event Related Phase cross-Coherence*
- *ERP – Event Related Potential*
- *ERPCOH – Event Related Phase cross-Coherence*
- *ERS – Event Related Synchronization*
- *ERSP - Event Related Spectral Power/Perturbation*
- *FFT – Fast Fourier Transform*
- *fMRI – functional Magnetic Resonance Imaging*
- *GABA – Gamma Aminobutyric acid*
- *Glx – Glutamate*
- *ICA – Independent Component Analysis*
- *IPSP – Inhibitory Postsynaptic Potential*
- *MEG – Magnetoencephalography*
- *NF-1 – Neurofibromatosis type-1*
- *PET – Positron Emission Tomography*
- *PFC – Prefrontal Cortex*

# List of Figures

# Summary

This thesis is divided in four main parts:

Chapter one describes the state of the art. Here, I will briefly introduce some theoretical aspects of biological processes and its relations with electroencephalography.

Chapter two, summarizes the methodology employed, including all scripting processes and algorithm creation process. Considerations about pre-processing, the time-frequency image calculation and the exploratory data analysis.

Chapter three will focus on results about all previous created scripts and routines for the evaluation of electroencephalographic oscillatory signatures and the relations between hemodynamic functional brain signals and inhibitory neurotransmission.

Chapter four contains the conclusions of the work performed and final considerations about all explored matter.

# Contents

# 1 Introduction

## 1.1 Theory about oscillations

### 1.1.1 Neural cells

The human central nervous system (CNS) is by far the most complex of all systems that constitute the human body. It is responsible for a centralized control of behavior as well as control of different organs either through electrical activity or hormone secretion.

The CNS is composed of neurons and supporting cells. The first type of cells, neurons, are characterized by the ability to respond to a stimuli with an electrical discharge called nerve impulse or action potential. The glial cells are in charge, among other functions, of support functions, isolating neural processes, controlling the environment around and taking part in repairing methods[1], in short, ensuring the homeostasis of the brain.

Neurons are composed of axon, dendrites and cell bodies. Cell bodies contain most of the nerve cells' organelles. Axons are long cylindrical cellular extensions, which transmit electrical impulses, sometimes through long distances (e.g. over 1m). Dendrites are responsible for the connection to either the axons or dendrites of other nerves or relay the signals to other nerves. Each neuron is connected with thousands of nerves due to dendritic connections, creating dense networks of signals[2,3], each one carrying information previously integrated, converting brain into a complex electrical signal networking[1,2]. Pyramidal neurons (Figure 1, specific type of neurons localized in the cortex) have especial role on production of macro electrical signals, since their activity cause the main source of electroencephalogram (EEG) activity[4].

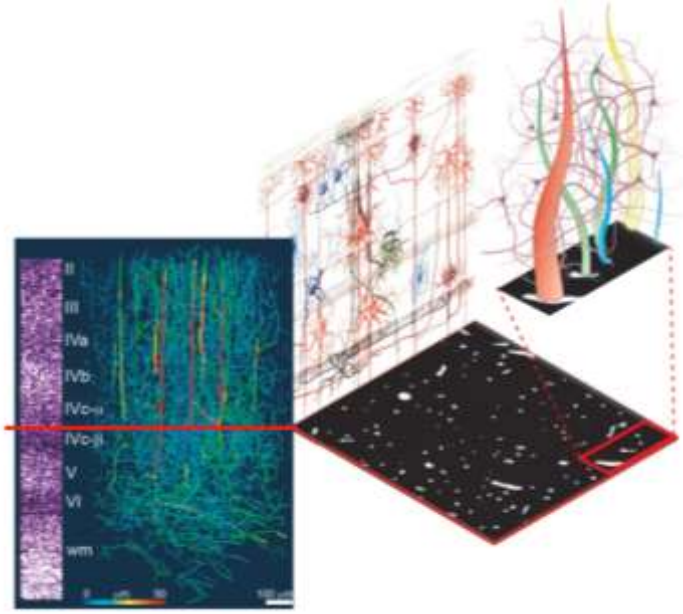


*Figure 1 – Relative density of pyramidal cells and vascular network[5]. Pyramidal cells are responsible for the creation of a dipole on the brain cortex, a great generator of EEG signals[6]. Shaded square represents an fMRI voxel and, in white, space occupied by vessels.*

### 1.1.2 Neural activity

Activity in CNS is related to the existence of currents transferred between functional junctions between dendrites and axons or dendrites and dendrites, a phenomenon called synaptic signaling. Normally, in nerve cells there are a resting voltage around 60-70 mV with negative polarity in nerve cells. This potential may change with synaptic activity. If the action potential travels along the fiber, which ends in an excitatory synapse, an excitatory postsynaptic potential (EPSP) occurs in the following neuron, called the post-synaptic potential. If multiple EPSP's end in the same neuron, there will be a summation of signals, producing an action potential in the following neuron, if the threshold is reached. If the action potential culminates in an inhibitory synapse hyperpolarization will occur, creating an inhibitory postsynaptic potential (IPSP) (Figure 2).

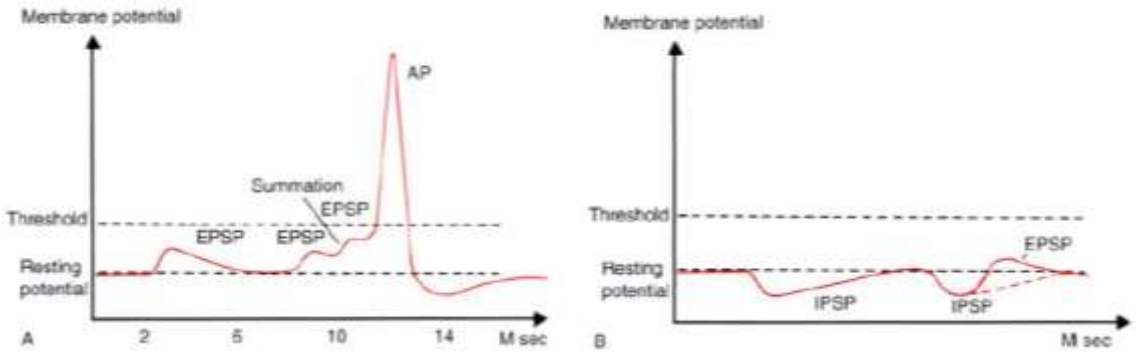


*Figure 2 – On the left, summation of EPSP triggering an AP. On the right, hyperpolarization of the neuron. The probably of cell to fire an AP is diminished.* [1]

The information transmitted by a nerve cell is called the action potential (AP). APs are caused by an exchange of ions across the neuron membrane and an AP is a temporary change in the membrane potential that is transmitted along the axon. The membrane potential depolarizes, producing a spike. After the peak of the spike, the membrane repolarizes. The potential becomes more negative than the resting potential and then returns to normal. The action potentials of most nerves last between 5 and 10 milliseconds.

Different types of stimuli induces membrane depolarization, which can lead to AP initiation. Sensory nerves respond to many types of stimuli, such as chemical, light, electricity, pressure, touch, and stretching. On the other hand, the nerves within the CNS (brain and spinal cord) are mostly stimulated by chemical activity at synapses. Very weak stimuli cause a small local electrical disturbance, but are not sufficient to depolarize the neuron up to the point of producing an AP. As soon as the stimulus strength goes above the threshold, an action potential is started and travels down the nerve, ending the synapse[7].

Normally, a neuron integrates information arriving from many other neurons[1], which ends up eliciting or not a response in terms of depolarization (Figure 3), depending on the sum of the synaptic input it receives. Total synaptic input means the sum of both excitatory and inhibitory synaptic influences received by the neuron[7]. A great example of synaptic integration is the sensation of pain: spinal cord mediates information about a painful stimuli. While a strong input is received from the sensory neurons reacting to the painful stimuli, high level integration factors concerning, for example, the state of

mind and other contextual variables are also taken into account. All the integrated information results in different degrees of perceived pain.[1]

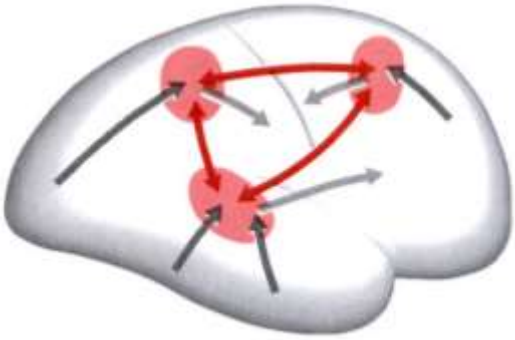

*Figure 3 – Distributed neural networks. Communication between distant neural networks is depicted. An example of this type of long range communication is the sensation of pain*

At birth, the human brain has approximately $10^{11}$ functional neurons, which corresponds to a density of $10^4$ neurons per cubic mm. This massive density allow a measurable quantity of synapses generating recordable macro signals.

Although neurons are the central unit in the nervous system, they are only relevant in the network where belong. In truth, a neuron can only be understood in conjunction with the thousands of neurons that communicate to it through synapses[1,2,8]. However, this huge number of interconnections is not enough to explain the complexity of processing achieved by the human brain. Thus, other mechanisms of neuronal computation and large-scale integration are hypothesized, such as, for example, integration through oscillatory activity.

### 1.1.3 Brain oscillations

Despite the large number of brain oscillations documented, there are still no classifications unanimously accepted. A useful taxonomy of brain oscillations would require that each individual oscillatory classes represent physiological entities generated by distinct mechanisms. The same mechanism giving rise to different frequency bands in different species or the same species ought to be referred by the same name, even though the dynamics underlying the rhythms may be different[9] (Table 1). Unfortunately, the exact mechanisms of most brain oscillations remain unknown.

*Slow oscillations of Up and Down states (<1 Hz)* are the overriding EEG pattern during non-REM sleep. During this time, all the cortex cell types are switching between

depolarization and hyperpolarization. Recent works link these phenomena to memory consolidation processes[10].

*Delta oscillations (1-3Hz)* are present during normal sleep. They are characterized by the high amplitude waves. There is a link between some cognitive functions and delta waves, as seen by the increase of amplitude of delta waves in oddball experiments, for example[11–13].

*Theta oscillations (4-7Hz)* are prominent coherent oscillations observed in the hippocampus and its surrounding limbic structures during exploratory movements. In humans, the theta rhythm was found to be enhanced in a variety of neocortical sites during working memory, for example when a subject was required to remember a list of items across a delay of a few seconds. The theta rhythm appears to be particularly prominent in the frontal midline (including the anterior cingulate cortex), a sub region of the prefrontal cortex (PFC) implicated in behavioral monitoring, evaluation of response outcomes and other aspects of cognitive function. It is functionally connected with attention and memory processes[2,11–15].

*Alpha oscillations (8-12Hz)* are involved in attention, awareness and inhibition. The alpha rhythm remains a model to analyze clinical EEG. Oscillations can be visualized when eyes are closed, whereby alpha desynchronizations, i.e. decreased alpha activity, in occipital areas are related to an increase of the visual processing[11,12,16–21].

*Beta oscillations (13-30Hz*) along with gamma rhythms have been recorded in association with attention, perception and cognition. Normally they increase with mental activation, but can also appear during drowsiness or light sleep. The power of beta waves decrease at the onset of movement execution suggesting their relation to an idle state of the control of the motor system[2,21,22].

*Gamma oscillations (30–200 Hz)* are found in different regions in brain like prefrontal areas, hippocampus, neocortex, primary visual cortex and are associated with many cognitive functions.

*Table 1 – Known sources of oscillations and respective functions.* [3]

| | Delta (1-3 Hz) | Theta (4-7 Hz) | Alpha (8-12 Hz) | Beta (13-30 Hz) | Gamma (30-200 Hz) |
|---|---|---|---|---|---|
| **Anatomy** | thalamus, neocortex | hippocampus, sensory cortex, prefrontal cortex | thalamus, hippocampus, reticular formation, sensory cortex, motor cortex | all cortical structures, subthalamic nucleus, basal ganglia and olfactory bulb | all brain structures, retina and olfactory bulb |
| **Function** | memory, synaptic plasticity | memory, synaptic plasticity, top-down control and long-range synchronization | inhibition, attention, consciousness, top-down control and long-range synchronization | sensory gating, attention, motor control and long-range synchronization | perception, attention, memory, consciousness and synaptic plasticity |

### 1.1.4 Gamma waves and binding problem

The last advances with gamma waves suggests that gamma waves are related to processes of synchronization[2,23–26] and integration of sensory information[27,8]. Gamma oscillations started to attract major interest when they were shown to correlate with perceptual binding. In the cat visual cortex, it has been demonstrated that synchronous firing of neurons at frequencies in the gamma range is associated with feature binding. When two neurons are driven by one visual stimulus which extends across both their receptive fields they tend to fire in synchrony. If, however, the two neurons are activated by different objects they tend to fire asynchronously (Figure 4)[23,24,28].

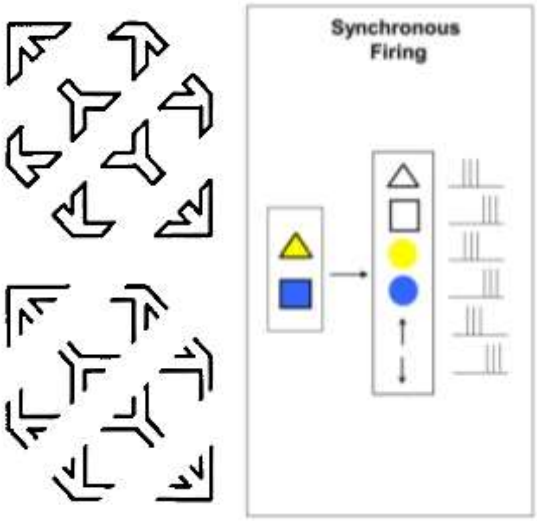


*Figure 4 – On the left, gestalt principles of perceptual grouping: The diagram on top seems to be a collection of unrelated objects. Below, removing subset of the lines, a clear relation between objects and the Neckar cube is revealed.*[29]*. On the right, a scheme of the classical hypothesis about the binding problem, where neurons responding to features of the same object would tend to synchronize* [30]

Gamma activity band (above than 30 Hz) has been associated with many stimulus-induced cognitive functions namely memory[11,12], perceptual binding[30], attention and object recognition[31]. It can also represent an attractive solution for the binding problem due to the time scale characteristics ($\frac{1}{30}$ seconds of minimum time resolution for encoding mechanisms).

Due to the gamma band being a broadband, different sub-bands were identified and reported in a variety of studies[32,33,34], including studies of electrocorticography(ECoG), where frequencies reaching 500Hz are found[35].

The last forty years of research have shown that the binding problem cannot be solved easily. It arises from a fundamental problem: how the brain puts together information about a single object that is processed in distinct brain regions. Binding by synchrony theory states that separated assemblies of cortical and subcortical neurons, coding different characteristics of a same object (like shape, color or position) fire synchronously, combining information and interacting through long distances.

However, this wide range of frequencies rises a classification boundary problem when an independent data-driven validation approach is carried out. This information will be analyzed in the next chapters.

## 1.2 Technical considerations on Electroencephalography

The investigation of oscillations in neurosciences in humans began when Hans Berger (1873-1941) assigned the observed large-amplitude rhythm to waves with a named frequency of 10 Hz (alpha waves because they were the first to be observed), induced by closed eyes, during visual rest. He named the faster, smaller amplitude waves, present when the eyes were open, the beta waves[9].

Studies of electroencephalography (EEG) in humans began in 1924 with Hans Berger's works. In that period galvanometers were used to record currents, in a non-invasive manner[36].

EEG is a powerful neurophysiology technique and based on Hans Berger's seminal work about the brain, there is the possibility to investigate patterns of activity in the normal and diseased brain

When one is concerned to investigate phenomena with fast dynamics, EEG is a great choice, due to high time resolution. It has advantages like the size and price of equipment, tolerance to movements and low auditory noise production, which is important when demanding tasks are required. However, it has low spatial resolution, poor signal-to-noise ratio it is difficult to measure data from deep areas of the brain, unlike other neuroimaging techniques like functional magnetic resonance imaging (fMRI) or positron emission tomography (PET). On the other hand, these techniques have poor temporal resolution. Best results can be achieved using multimodal techniques like EEG/fMRI, EEG/MEG (magnetoencephalography) or EEG/PET.

As described before, cortical neurons and their synaptic activity are the main source off EEG signal. The Pyramidal cells are all arranged in the same orientation allowing the production of an electromagnetic field. Primary transmembranous currents in axons generate secondary ionic currents along the cell membranes in the intra- and extracellular spaces[36]. The portion of these currents that flows through the extracellular space is directly responsible for the generation of field potentials. So, scalp EEG signals are produced by partial synchronization of neuronal scale field potentials. The flow of the electrical potentials over the scalp is also known as volume conduction.

The field potentials are recorded by EEG in the scalp after crossing the main layers with considerable resistivity (Figure 5) of the electric signal, being the skull the most relevant resistivity (approximately 177 Ωm) compared with the brain and even the scalp.

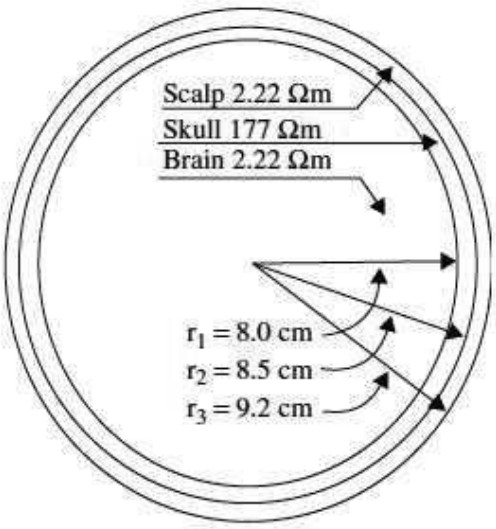


*Figure 5 – Scheme of the brain resistivities[7].*

A crucial point when acquiring data is their placement and resistivity. Different types of electrodes can be used, namely saline-based electrodes, disposable electrodes or headbands with electrode caps. To enable a satisfactory recording the electrode impedances should read less than 5 kΩ and be balanced to within 1 kΩ of each other. For more accurate measurement the impedances should be checked after each trial[7].

### 1.2.1 Acquisition

EEG signaling sampling should in general not be below 500Hz. By the Nyquist criterion, for this value, sampling bandwidth will be, ate least, the half of that value (250Hz).

The most used electrode setting is the so called 10-20 system (Figure 6) recommended by The International Federation of Societies for Electroencephalography and Clinical Neurophysiology[7]. Some specific configurations can be adapted based at this convention (namely for BCI applications).

Filtering process can be applied before or after acquisition, and processes include filtering and artifact rejection algorithms in order to extract artifacts such as line noise at 50Hz, eye movements and blinks.

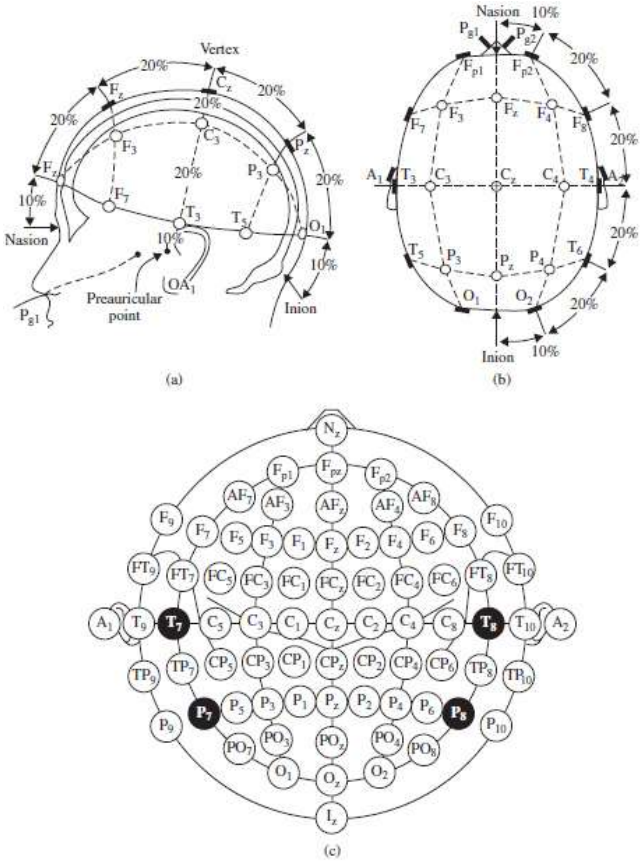


*Figure 6 – 10-20 International electrode placement system*

### 1.2.2 Analysis

Oscillations, in general, can be described as evoked, induced or spontaneous activity[31]. The last one is not relevant for studies focusing on task related brain activity and will not be considered here. Evoked oscillations are time-locked and phase locked to an event. Induced oscillations are time-locked, but it are not phase locked to an event[26,37–39].

There are some different approaches to the matter and some analysis techniques can be used depending on the purpose to reach.

#### *The Event Related Potential technique (ERP)*

Early uses of of ERP (Figure 7) in cognitive neuroscience focused on the speed and accuracy of motor responses and sensory "bottom-up" responses[40]. ERP is able to record "evoked" and spontaneous activity deriving from mixed cortex sources, due to the poor spatial resolution. Reverse is also true: one source can contribute to generate various

peaks in the ERP waveform. In short, these scalp signals represent EEG signal locked or not to an event and averaged across trials.

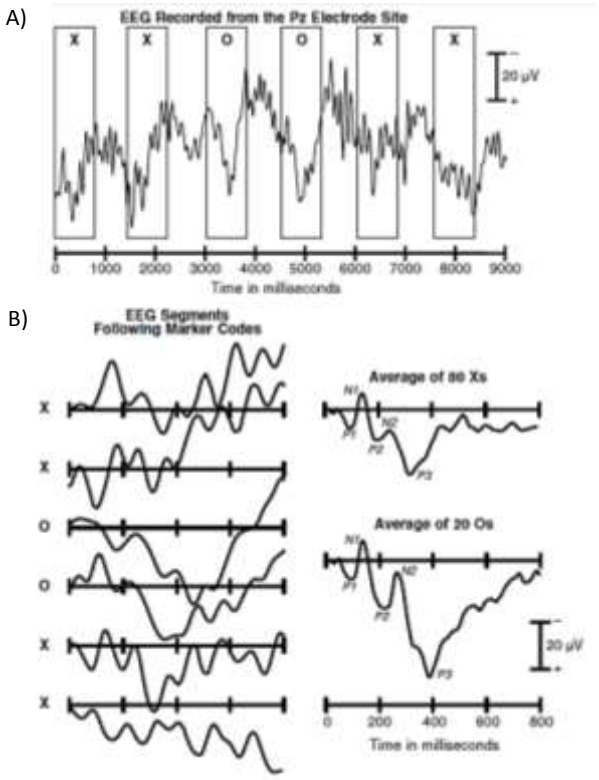


*Figure 7 – Example ERP experiment[40] – A) Subjects viewed sequences consisting 80% of X's and 20% of O's. EEG signals shown. B) For each segment, ERP is associated to a letter to proceed to the average of trials and get the final ERP.*

### *Time-Frequency analysis*

In modeling event-related activity in the ongoing EEG, amplitude and phase effects may be considered separately or in combination.[38] The event related spectral perturbation (ERSP)[38] reveals aspects of event-related brain dynamics not contained in the ERP average of the same response epochs. The ERSP measures average dynamic changes in amplitude of the broad band EEG frequency spectrum as a function of time relative to an experimental event. That is, the ERSP measures the average time course of relative changes in the spontaneous EEG amplitude spectrum induced by a set of similar experimental events.

Phenomena like event-related desynchronizations (ERD) and synchronizations (ERS) can be depicted at 2 dimensional images (frequencies (Hz) along time (ms)). The software used along this work was EEGLab, that computes each pixel value as being the

power( in dB) at a given frequency and latency relative to the time locking event (Figure 8)[41].

Back to the basics of EEG and its multichannel recordings all over the scalp, it will be intuitive but not trivial to analyze the consistency between pairs of electrodes in an attempt to address the brain's regional connectivity and interregional interaction[42]. Cross coherence analyze provides the relation on phase between pairs of electrodes averaged by trials to determine the degree of synchronization between two activity measures[43]

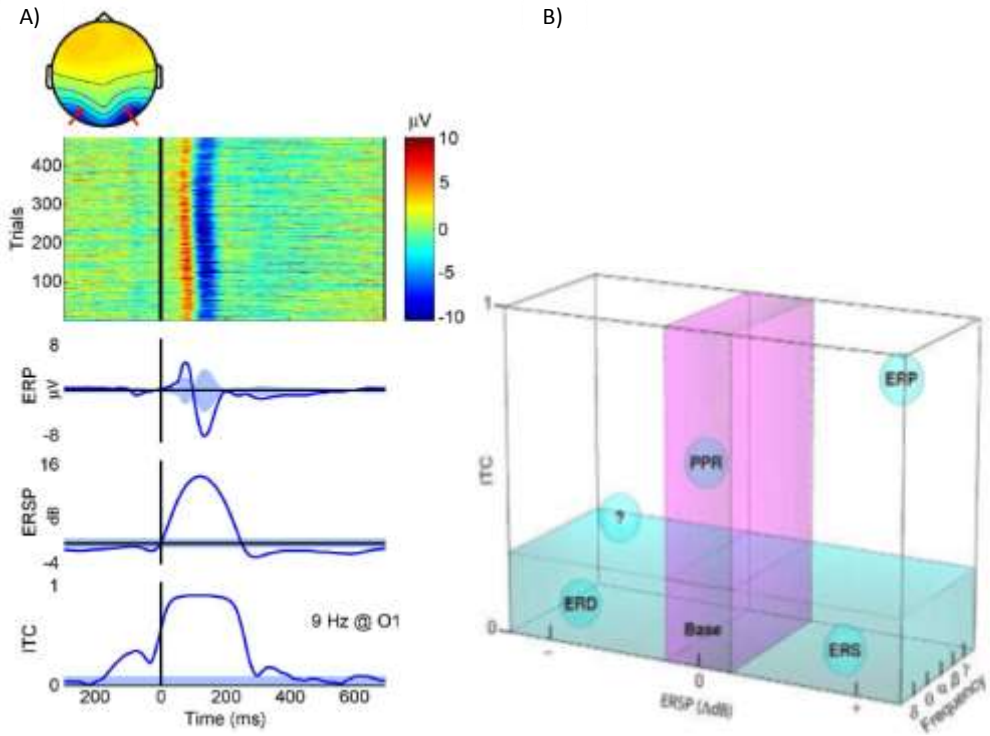


*Figure 8 –A) Information depicted in different perspectives: averaged trials in the time component, ERP from the averaged trials, ERSP and Inter trial Coherence (ITC) along the time courses. B) Event-related brain dynamic state space: ERSP image (Power (ΔdB) vs Frequency (Hz)), containing synchronizations (ERS) and desynchronizations (ERD), with partial phase resetting (PPR). ERP representing evoked activity with strong phase locking and power increase ("?"Representing opposite of ERP).*

## *Independent component analysis*

Independent component analysis (ICA) is a statistical linear decomposition of data. When data is acquired, there are volume conduction problems, causing redundant information over proximal acquisition areas. ICA algorithm maximizes the independent component of a set of sources[31]. An important application of ICA is in blind source

separation (BSS), an approach to estimate and recover the independent source signals using only the information of their mixtures observed at the recording channels[7].

## 1.3 BOLD

In response to variations of activity on neural tissues, different quantities of oxygen or glucose have to reach active areas. The hemodynamic response is related to the influx of oxygen, and the respective changes in oxyhemoglobin vs. desoxyhemoglobin levels lead to changes in the T2* magnetic ressonance signal, the so called BOLD signal. Blood Oxygen Level-dependent Hemodynamic (BOLD) fMRI imaging is a method to observe areas with higher oxygen perfusion, which can be linked with brain activity. What is still incognito is how that neuronal activity is influenced by the amplitude of the hemodynamic responses, and vice-versa. In Particular, investigations have been performed in a way to verify the existence of a relation between neural oscillations and hemodynamic responses.

## 1.4 Magnetic resonance spectroscopy

MRS can collect information about metabolic state of the tissues and it's largely used in the study of brain tumors, stroke or Alzheimer's disease. Spectroscopy is too the only in vivo tool capable of non-invasively measure brain metabolites[44]

## 1.5 Project motivations and objectives

Actually, the study of neural has been actively developing in the fields of clinical neuroscience, including diseases such as diseases like schizophrenia[2,42,45], epilepsy and neurofibromatosis [16], impaired brain states (like alertness[21], coma or brain death[13]) and neuroengineering areas such as brain computer interfaces[20,46,47] (BCI).

A very active topic of discussion today is the classification of oscillations. What is the cutoff frequency of beta waves? Will there be any genetic fingerprint in the frequency characteristic bands? Are there many subtypes of gamma bands? How can one define band boundaries?

These are some questions that current neuroscience is trying to answer. It is essential to know what biological processes trigger different frequency bands and which information can be transmitted by those bands and if they converge with the binding theory[9,27,11,12].

This thesis will explore an important area where seems to be some controversy, divergent analyses and approaches. Discussed topics with different answers are appearing, like the undefined limits and functional interpretation of gamma band patterns or else the existence or absence of relation between gamma frequencies and GABA concentrations, which are thought to regulate their frequencies. This is a very difficult task, due to the large variability of oscillation sources and the difficulty to know what sources produces what oscillations and the way genetic background different marked sub-bands.

One another goal to achieve is to use acquired data and create automated exploration and data-driven algorithms, allowing to segment gamma sub-bands and trying to find correlations between gamma peaks obtained by our approach and GABA concentrations, attempting to confirm one of the parts.

The thesis also aims to test a clinical neuroscience question using time and phase synchrony methods among control group and neurofibromatosis type-1 group, where it is important to exploit differences in synchrony, as observed in other genetic neurodevelopmental syndromes such as Williams syndrome.

# 2 Methods

This methods chapter is composed by a description of all processing steps as well as of all created algorithms and scripts that were used to process entire set of data.

For all data processing were used functions from EEGLab (v12.0.2.5b) running in Matlab® R2012b.

## 2.1 Preprocessing

Preprocessing of data is a crucial step for a successful and appropriate analysis. EEG signals are contaminated by environmental and in particular line noise, as well as movement and blink artifacts. The main approach in the preprocessing stage are the noise and artifact removal steps, but is also decisive to apply adequate processing of the raw data, concerning the type of stimulus, the frequency of acquisition and the type of design to be followed.

A great goal to achieve would be the standardization of a preprocessing model that allows faster and automatic preprocessing of EEG data with a reliable precision.

### 2.1.1 Down Sampling

Most of times, the acquired data has more resolution than needed and, when working with large quantity of data, there's a need to reduce the processing time. In this work, evaluation of frequency components does not exceed 100Hz so, by the Nyquist criterion, where $f_{sampling} = 2f$, being $f$ the highest frequency considered in the analysis (100Hz), a sampling frequency of 200Hz is enough, but 250Hz is normally recommended. In this work, we used down sampling to 400Hz. EEGLab® uses the *resample()* Matlab® function that applies an anti-aliasing (lowpass) FIR (finite impulse response) filter to the original raw data during the resampling process. The integrity of data is conserved and the saving time is significant.

### 2.1.2 Band pass filter and notch filter

The purpose of this work is to evaluate neural oscillations at the scalp level in a range between 5 and 100Hz while removing the line noise at 50Hz with a notch filter between 47.5Hz and 52.5Hz (Figure 9). This point is not critical to the data evaluation, so the properties of filter are not further analyzed.

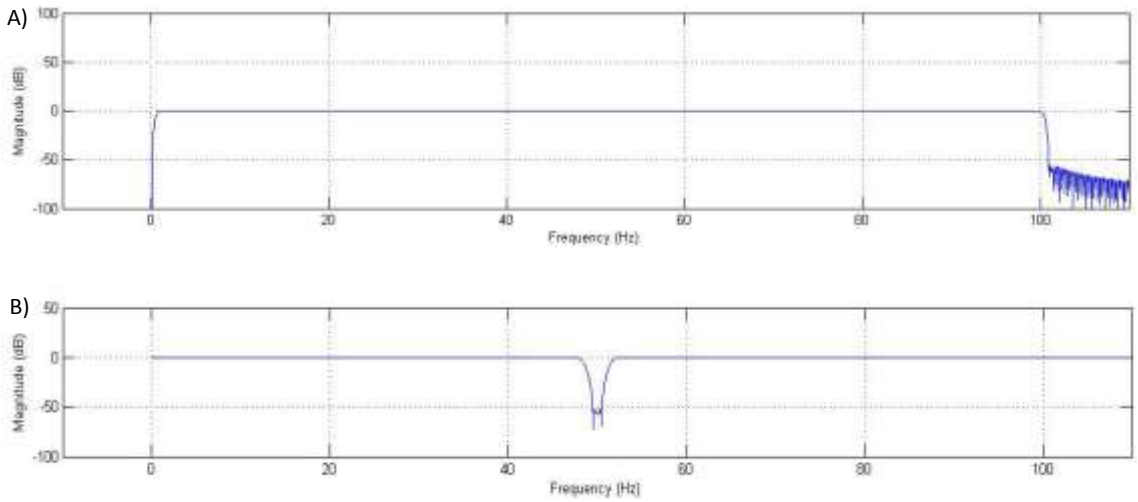


*Figure 9 – A) Band pass filter applied to data. Filter order/transition band width is estimated with the following heuristic in default mode: transition band width is 25% of the lower pass band edge. B) Notch filter around 50Hz.*

### 2.1.3 Epochs

Due to EEG technical features, it is important to record a large number of trials and proceed to the average of the same, excluding noise and relevant artifacts. According to the experimental protocol, volunteers repeat a specific task $n$ times (in this work, $n$ =100). Epoching triggers are chosen according to experimental protocol in order to get $n$ times the same neural response from volunteer. In this work there are two triggers with special importance. The trigger "10" (marked below in red) manifests the start of stimulus, while trigger "20" marks the end of the stimulus (Figure 10). Other triggers like the response of the subject are not relevant for the analysis of the problem, because we will analyze brain variations to sensory visual stimulus presentation.

All channel data was referenced for CPZ channel.

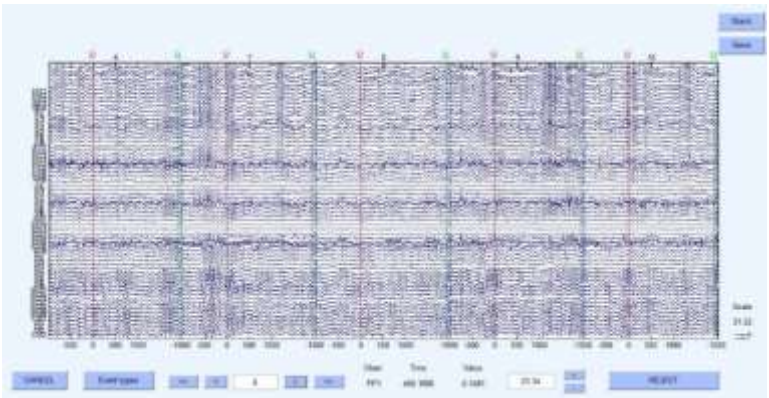

*Figure 10 – EEGLAB channel scroll window after epoching. Time periods were locked to trigger "10", indicating the beginning of grating stimuli. Trigger "20" indicates the end of grating stimuli in the periphery of visual field.*

*Visual stimulus and task*

Visual stimuli (Figure 11) consisted of a circular moving grating (80% contrast, spatial frequency 2 cycles/degree, 4° diameter, velocity 1 degree/second), with equal luminance to the background. Stimuli were presented in the lower left visual field, subtended 4° horizontally and vertically, with the centre of the stimulus located 3.3° from a central fixation point. Stimulus duration had random interval time (between 1.5–2 s) followed by 2 s of fixation point only. Participants were instructed to maintain fixation on the central point for the entire experiment and to press a button, in the shortest reaction time, when the grating disappeared

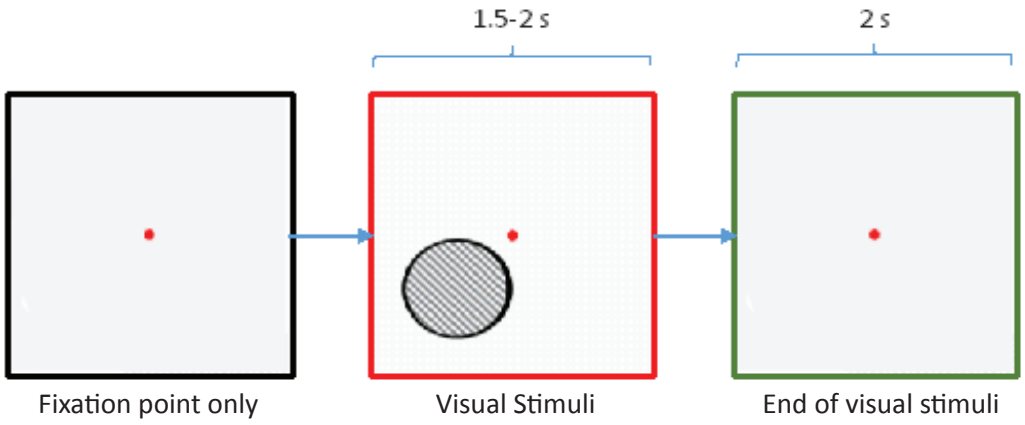


*Figure 11 –Visual task diagram (courtesy of Maria Ribeiro)*

### 2.1.4 Artifact rejection

A common way to reject artifacts is by visual inspection. The main processing principle of this thesis was to automate the processes of analysis, particularly in the preprocessing stage. In order to perform the inspection automatically, some simple methods were applied. Based on channels information, namely VEO and HEO channels, there is a possibility to recognize blinks through voltage peaks. Blinks have a known pattern in EEG, reaching potentials of more than absolute 100 microvolt. An EEGLab built-in algorithm identifies epochs where there are blinks and it is also possible to remove them. This artifact rejection proved to be viable method on major artifacts removal. After these steps, more than 80% of data were ready to use to analysis.

## 2.2 Time-Frequency image calculation

Time frequency calculations will approach essentially two components: ERSP images and channel cross-coherence.

Calculating an ERSP (Figure 12) requires computing the power spectrum over a sliding latency window then averaging across data trials. For a certain number of trials *n*, being $F_k(f,t)$ the spectral estimate of trial *k* at frequency *f* and time *t:*

$$ERSP(f,t) = \frac{1}{n}\sum_{k=1}^{n} |F_k(f,t)|^2$$

EEGLAB function *crossf*() computes event related coherence (ERCOH) between two channel or component activities in sets of trials to determine the degree of synchronization between the two activity measures. Here, only phase cross coherence (ERPCOH) will be used. It estimates the extend of complex linear relationship between the two signals. For $b$ and $d$, different EEG channels, being $F_k(f,t)$ the spectral estimate of trial *k* at frequency *f* and time *t*:

$$ERPCOH^{b,d}(f,t) = \sum_{k=1}^{n} \frac{\sum_{k=1}^{n} {F_k}^b(f,t){F_k}^d(f,t)^*}{|{F_k}^b(f,t){F_k}^d(f,t)|}$$

### 2.2.1 Storage model constraints

The algorithm for time frequency requires computational power, especially when computing ERPCOH, when output final matrices reached 5 GB of data (Figure 13)(for the current work) and the number of different images, $n_{subjects}.\frac{{n_{channels}}^2}{2}$ (165292 images if computed cross coherence between all channels), forcing a somewhat intricate structural organization of the data.

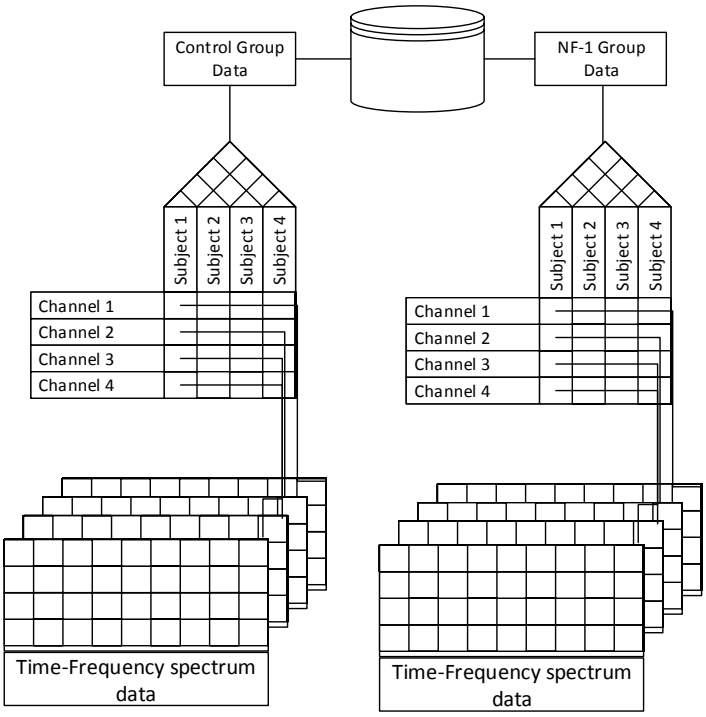


*Figure 12 - Diagram showing used data storage model for time-frequency spectra. Main structure groups all information, divided by groups. Each group structure concenters all time-frequency matrixes.*

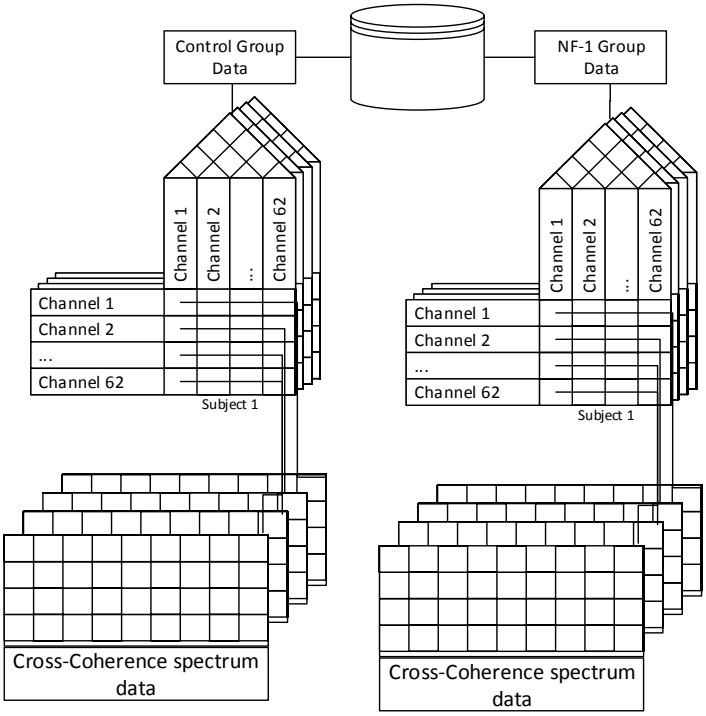


*Figure 13 - Cross-coherence main structure*

### 2.2.2 Normalizations, statistics and other techniques

To visualize the event-related power changes in a meaningful way, a normalization with respect to a baseline interval must be performed. EEGLab allows some methods of image normalization. For example, one way is division from baseline, for each frequency corresponding to the average power in a baseline interval from all other power values. This gives, for each frequency, the absolute change in power with respect to the baseline interval (in terms of ΔdB). There are some other normalizations approaches like standard deviation from baseline or z-score from baseline.

In this analysis, we used division from baseline (the default EEGLab baseline normalization).

There are also combinations of scale and unity representations that we must take in account when processing data. In terms of data visualization it can be useful use logarithmic scales but, when computing threshold images, this fact must be taken in account

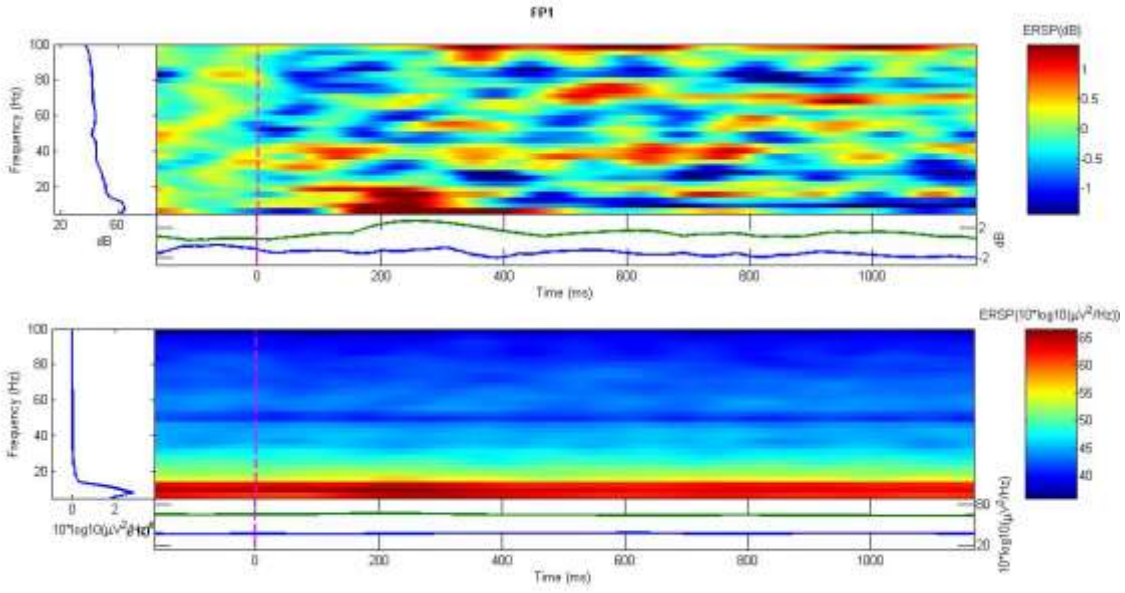


*Figure 14 – Above: Normalized ERSP with divisible baseline. Alterations of power comparing to baseline. Below: There is no normalization relative to the baseline and significant changes along the time axis are not seen. Both power scales are in a logarithmic scale. As we talk about energy spectral density, we have unities like* $\frac{\mu V^2}{Hz}$ *or power unities(dB).*

In order to obtain more significant information, an important statistical tool can be used in the ERPS or ERPCOH signals: bootstrapping. Bootstrapping uses permutation statistics to attribute significance to an image part. In general, an algorithm randomizes the image and compares the image with other randomized images, filtering less

significant parts of the image. Despite the computational power required, bootstrapping may be one of the most adequate methods to use.

### *Discrete Fourier Transform and Wavelets*

Time-frequency calculation images have crucial relations with Fourier transforms and wavelets. When used, pure Fast Fourier transforms (FFT's) create results with severe loss of time resolution (potentially misleading when we're using EEG). On the other hand, pure wavelets decrease resolution in frequency and their use is not possible, especially when working with a large bandwidth (in this case, 5Hz-100Hz), given that the poor resolution at high frequencies implies loss of information (Figure 15). EEGLab uses a wavelet transform that increases the number of cycles reaching a percentage of cycles that would be used with FFT. Default values for wavelets are 3 cycles at starting frequency and increasing cycles up to 0.5 of total cycles for the same frequency if FFT were used. In this way, is possible to maintain relative integrity of data on time and frequency domains.

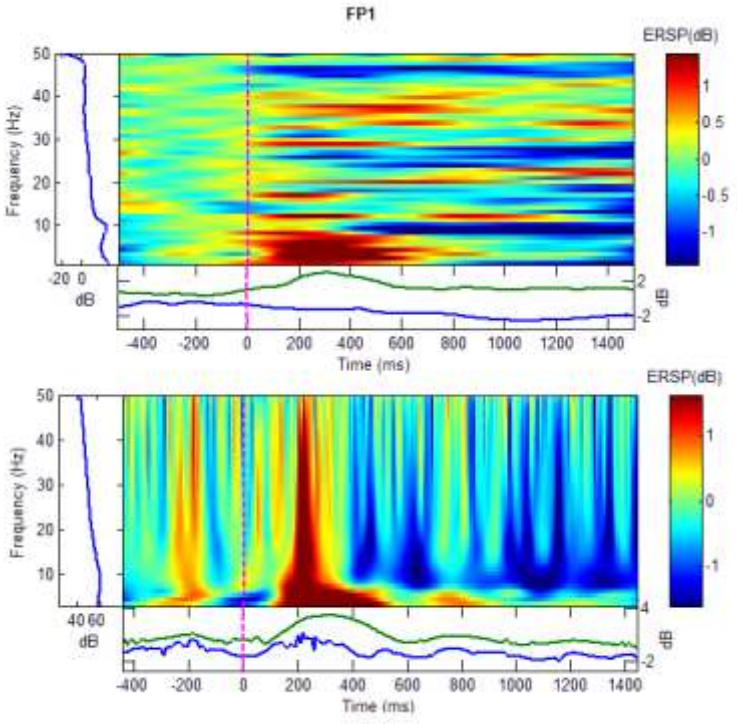


*Figure 15 - Above, ERSP calculated with FFT has strong loss of time domain integrity. Below ERSP calculated with Morlet wavelet with no increasing cycles. Morlet wavelet shows good integrity of frequency domain only on frequencies below 10Hz.*

## 2.3 Exploratory data Analysis

One of the most important objectives of the thesis is to analyze data in a data driven unbiased way. In the challenge to study data in a "blind manner", such a data driven method will be used.

### 2.3.1 First methodological approach

The first methodological approach (Figure 16)brings a general view of the analysis problems and starts to point the strategy to get information from preprocessed data. Below, the general scheme from this method exposes the critical points on the process. It starts with *Initial matrix Data* from both analysis groups and culminating with images from different bands for the two groups and some information relative to statistical differences.

The precise objective of this method is to achieve definition of the four band peaks on all frequency spectrum and compare results from different channels or clusters between groups. Some scripts used include standard Matlab® functions.

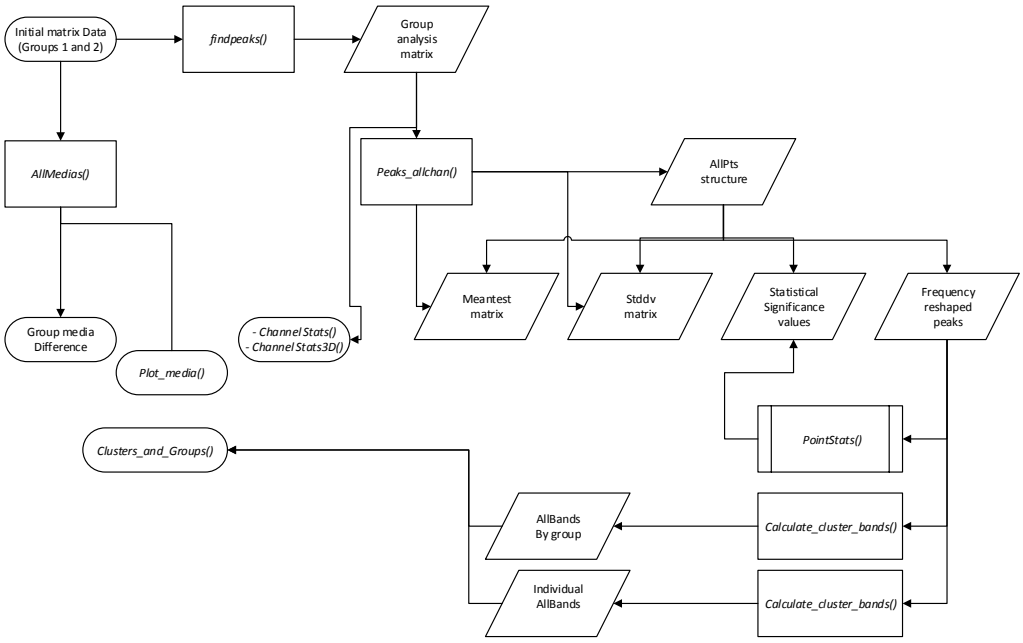


*Figure 16 – Schematic representation of first method of data evaluation. This image is also available in the annexes.*

### *Computation of time frequency power peaks*

ERSP spectra (Figure 17) of each trial are composed by a frequency by time axis, where each frequency has a timeline locked to an event. The first objective was to get simple statistics such as the average from subjects by group and by channel, verifying the existence or not of a marked and common oscillatory pattern for all subjects.

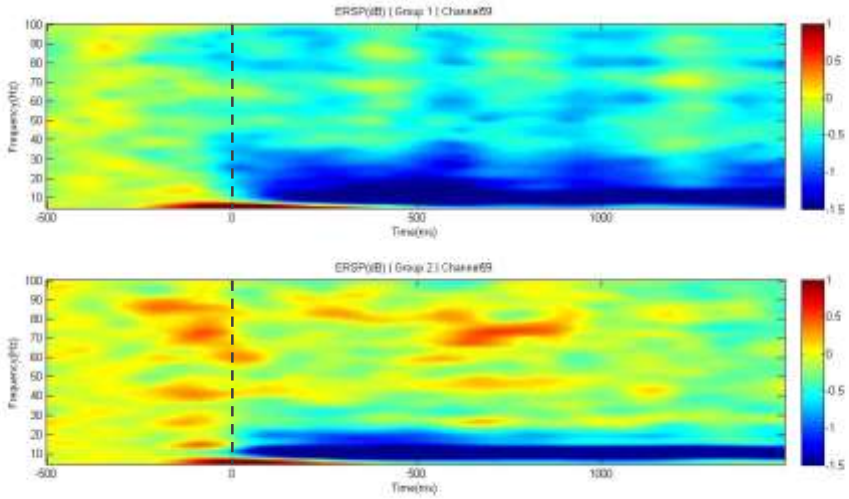

*Figure 17 - Event related spectral power image for each group in channel 59.*

### *Group analysis matrix and its generation*

The script to obtain the four main peaks of a time-frequency image is a key issue in all algorithms. The function only needs the main matrix to work. For each image in *Initial matrix data(i,j)* (being *i* the number of channels and *j* the number of subjects) the function will find the four main peaks and put them into another storage matrix, *analysis* matrix.

Constructing a matrix with this information allows to access anytime to the information of all peaks of all channels, as a comparison method or just like for the simple visualization of data. Starting with *analysis* matrix, there is a chance to explore all peaks by channel in one scatter map. The scatter map (Figure 18) plotted using *ChannelStats()* uses all the data from each channel to plot the information of the peaks by channel for each subject. *ChannelStats()* is one of the three main outputs the overall first methodological approach.

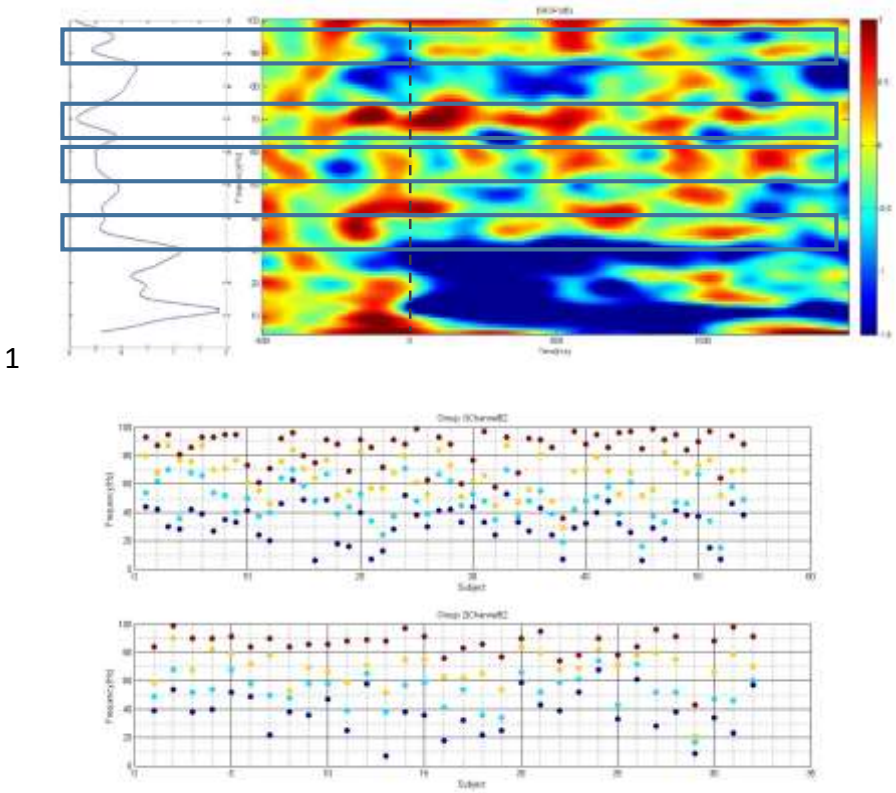

*Figure 18 – Above, identified bands, simply averaging times along all frequencies. Below, four found peaks of each participant along all frequencies.*

### *AllPts structure and bands output*

The next step is to look across the average of the peaks per subject and per channel, in order to investigate if there is any meaningful difference between groups. Some functions are used to fill the data in the *allpts* matrix, namely *Peaks_allchan()* and *PointStats()* functions. In this step, just a reorganization is done to all data and statistical tests are applied. Grand average by frequency peak is calculated along all subjects and final band of the matrix of average by group is displayed (Figure 19).

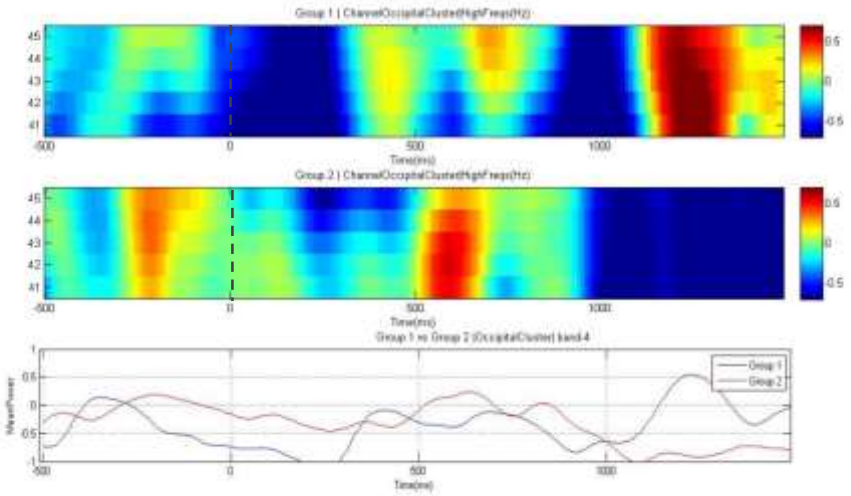

*Figure 19 – Comparison between cluster bands.*

### *Pros and cons of first methodological approach*

As a first approach into data evaluation, work done allows to determine that some directions must be taken instead of others. As described before, each subject tends to have characteristic frequency gamma bands. This factor helps to understand that the average into group might not, in the most of cases, show any significant result.

The process of finding peaks for each subject is not a data-driven method: we defined beforehand the number of bands to find across all frequency spectrum. Furthermore, the *findpeaks()* Matlab® function does not allow to choose parameters that may have special importance when bands are selected.

Using the average at each time point to calculate peaks will probably fail as well because of oscillatory characteristics of the waves: in certain times, is possible that the power decreases, which will not culminate in a peak when the average is calculated.

Due to all inconsistencies, this model will not be used to find frequency bands to correlate with GABA level however, it will be used for comparison between means of eventual existent sub-bands.

Despite all negative points, it was a decisive step within the scope of this project. It was a starting point for the next methodological approach, which will recycle some functions used in this model. It shows that oscillations classification problem is neither minor nor trivial.

### 2.3.2 Second methodological approach

One of the problems in defining of gamma bands automatically is that the spectral profile of the bands is empirically and arbitrarily described. There are no fixed parameters that can describe precisely what a gamma band is. Due these facts, the second method introduces criteria that can be adjusted for a better performance. As described about the ERSP images, is known that low frequency oscillations have more power, which requires a normalization of the data with a baseline.

We develop the algorithm (Figure 20) disposing of a z-score baseline correction but, by default, EEGLab uses the difference between baseline and the values of the data("To visualize power changes across the frequency range, we subtract the mean baseline log power spectrum from each spectral estimate, producing the baseline-normalized ERSP."[43]), which explains why this feature can be optional.

In general, in this method we will use a novel image based segmentation approach, taking advantage of the oscillatory properties of waves.

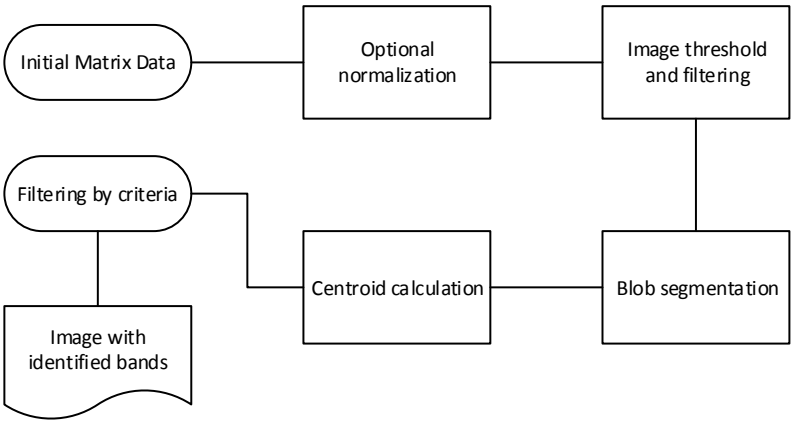


*Figure 20 –Second methodological approach scheme.*

#### *Thresholding and filtering data*

The basis of the algorithm lies on correct identification of *blobs,* regions of the image above of certain threshold (Figure 21), that demonstrate (in the case of ERSP images) higher power relatively to baseline, considered an important parameter to classify the bands.

The right threshold must be identified, and thereby this parameter still requires attention.

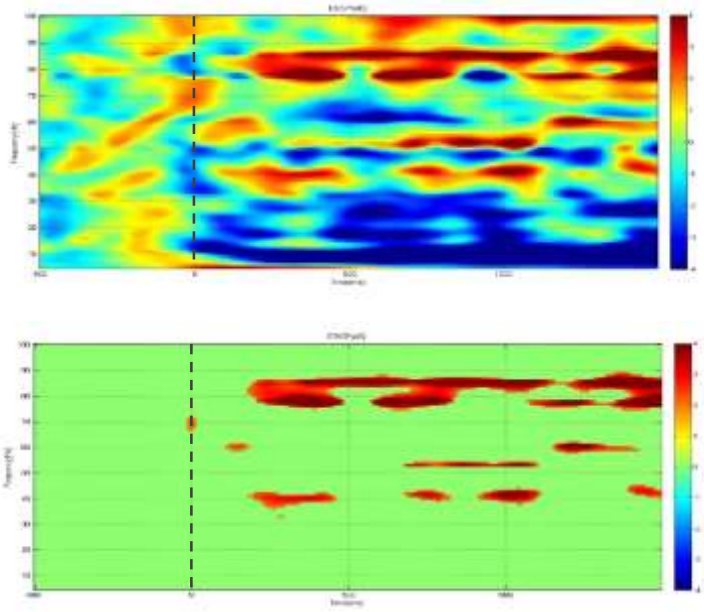

*Figure 21 – Comparison between ERSP images before and after thresholding.*

### *Blob segmentation script*

Part of this method seats in a particular strategy to select regions of interest by using blob segmentation. Implementation consists in taking the images at a certain threshold and to segment existing blobs, filtering the values of the image above a certain threshold. They will be considered the significant part of the image, which contributes to find gamma bands. At this point, some considerations are taken:

- A blob is a region from image containing a borderline with values all different of zero, and bounded by zero values.
- There's a minimum area to identify the blob;
- Blobs with considerable extension in frequency axes will not be considered.

In fact, in addiction, other filtering features could be implemented.

The main Matlab® functions for the script were *bwboundaries()* and *regionprops()*. These functions give a large number of options to characterize each ROI, allowing for the needed precise evaluation like area, perimeter, centroid, extreme points.

### *Centroid calculation script*

Like described before, the combination of the previous Matlab® functions give a powerful tool to analyze thresholded images. A great indicator of the center of the blob is the centroid. This parameter will be used to obtain the mass center of the binary bi-dimensional object. All centroid information combined is useful to proceed to blob clustering. Clusters following criteria described below will mark a frequency band (calculated by the average of each cluster blob centroids).

### *Criteria*

A set of criteria was made for the grouping of blobs by frequency or elimination if they didn't match to the specifications. Each blob has a centroid at frequency $f$ and a time $t$. The most basic criterion is the proximity between centroids. To belong to the same band, the blob cannot be distanced by more than 3 Hz, which means that absolute difference between the values of $f_{blob}$ can't be more than 3 Hz. The minimum number of blobs that are neighbors is two. Special case is taken when 1 blob alone has extension of more than 500 milliseconds. In that case, a single blob can form a band. When two or more blob centroids are in the same group, a rectangle is plotted with 7Hz height centered in the average of all $f_{blob}$ (Figure 22).

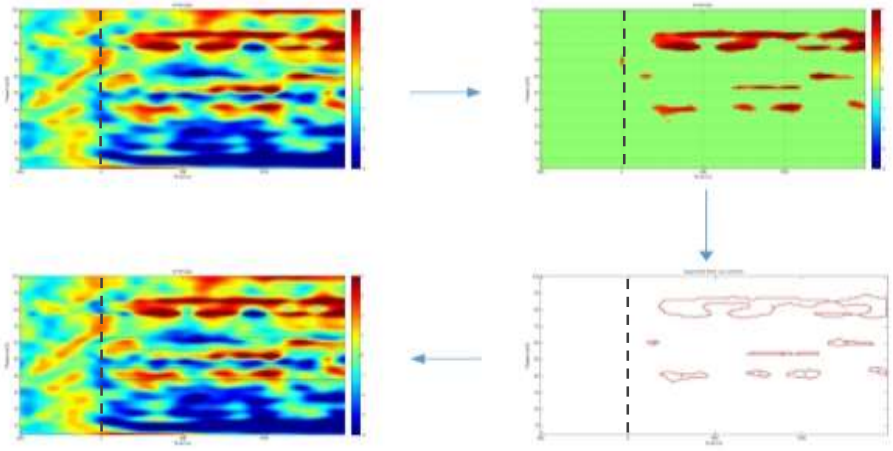

*Figure 22 -Step sequence for band identification.*

### *Method validation*

For the validation of the model for bands identification two experienced and independent researchers were asked to identify all the gamma bands presents in 20 random time-frequency ERSP images from left occipital channel, in a blind mode. Bands had to be identified on the peaks of frequencies in a window of ± 3Hz (Table 2Table 2 – Method validation. Number of bands identified by the algorithm with ± 5Hz window.). This value is arbitrary. Some practical studies in future may be important to define the precise values for the window of grouping peaks. For grouping, clustering methods could have been applied (like k-means), but we opted to make the own algorithm.

*Table 2 – Method validation. Number of bands identified by the algorithm with ± 5Hz window.*

| | Researcher A | Researcher B |
|---|---|---|
| Identified | 36 | 22 |
| Not identified | 28 | 12 |
| | 56,25% | 64,71% |

### *Pros and cons of the routine*

The obtained routine designed for band identification had good results and was more conservative when compared with the bias of experienced researchers. There is a reasonable difference between the quantities of identified bands among researchers, which is normal when visual inspection is used. However, with the implementation of standardized definition of band, these differences may be reduced.

Despite the low sensitivity at this step, the algorithm can be considered a good estimate of programmed calculated regions of interest, evaluating them in an unbiased manner. More than that, is one of the first steps looking for a parameterization of time-frequency bands. A data-driven model capable of find bands not only in EEG images, but might also be used in other modalities like MEG images.

### 2.3.3 Cross-coherence computation method

For the computation of cross coherence, the analysis method required a significant increase of processing time. For each of 86 datasets, we computed the relation between pairs of electrodes. At this time, I opted to process only half of scalp area (Figure 23), processing channels starting at channel number 30 (focusing on the visually responsive regions in the Occipital Parietal cortex). For each subject an inferior triangular matrix (21×21) was obtained.

To increase statistical power, clusters of channels were used (based on *Inês Bernardino et al.*[48]), averaging groups of channels by subject by group and obtaining clusters of data for each group.

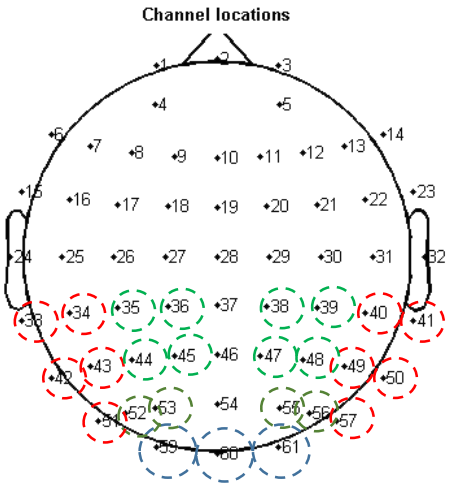


*Figure 23 - Groups of channels forming clusters. Center channels were not chosen to allow for comparisons between cerebral hemispheres (eventually between the same areas in each hemisphere).*

# 3 Results

## 3.1 Participants

The visual tasks were performed by 43 subjects divided in a control group (n=27; age=13 ± 3 (9-18) years old; F/M 17/10) and NF-1 group (n=16; age = 13 ± 3 (10-18) years old; F/M 13/4). Each participant performed the test twice (stimulus described previously), responding with the right hand for one run and the left hand for the other. Each run was composed of 100 trials.

## 3.2 ERSP results

### *Average group ERSP's do not show significant differences*

For the first general characterization, the grand average was calculated each group. Mean images show the subjects trends. Ideally, in the case of subjects manifesting activity in the same frequency ranges during an evoked or an induced response, a much more defined bands will be displayed in the ERSP mean images, while noise unrelated to the task will fade. In this experimental work, grand average images (Figure 24) show there are from the visual point of view no apparently significant differences between groups. In both the control and the NF-1 group, decreasing power in the alpha band is evident after the onset of the stimulus. However, there is no indication of common gamma bands across participants of each group. Whether this absence of gamma is the result of no activity related to the stimulus in this frequency band or as a result of an attenuation after averaging due to distinct narrow bands in different subjects, it remains to be explored.

In order to confirm the absence of striking differences observed by visual inspection of the averaged spectrograms, Wilkcoxon rank-sum tests ($p<0.05$) for each point of each spectrogram (Hz vs milliseconds) were performed. Bootstrapping statistics (n=200 permutations (default EEGLab number of permutations) and $p<0.05$) were already applied to each subject ERSP image, highlighting statistical significant data compared to baseline. No significant results were found, such as already suggested by visual inspection (Figure 24).

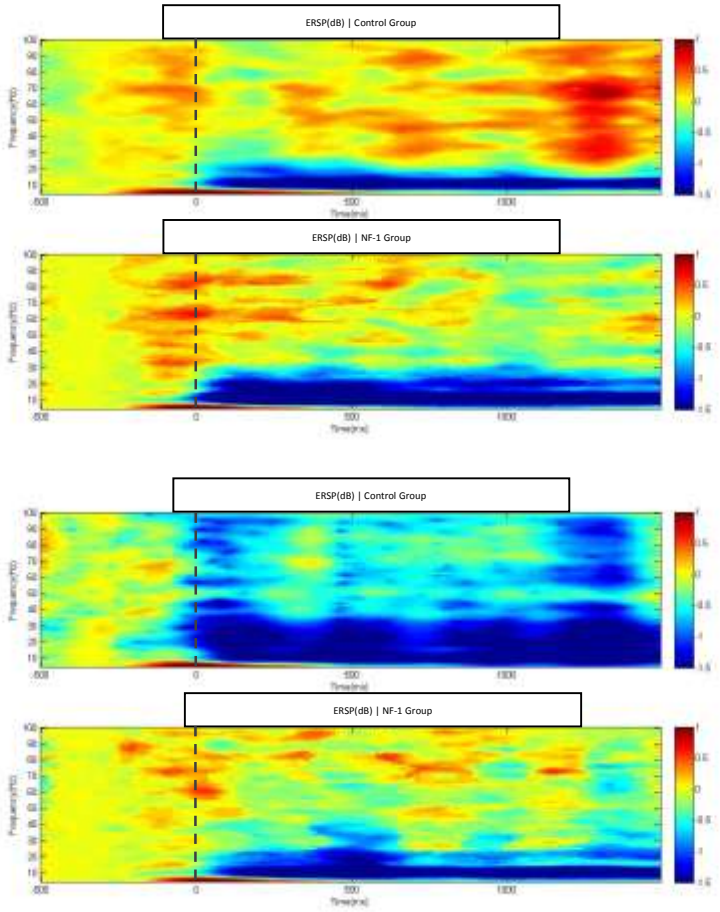


*Figure 24 – Examples of ERSP grand average across representative subjects of control (group 1) and NF-1 (group 2).*

## *Frequency peaks do not show significant differences between groups*

After concluding that the grand average of ERSP images does not evidence marked gamma band differences, the peaks of power for each participant were determined using the first methodological approach (2.3.1) with some corrections (i.e. the algorithm computes all the significant peaks above a minimum mean power, defined by the researcher). These alterations are applied together with bootstrapping threshold correction of images. The four most prominent peaks (in case they are identified by the algorithm) are plotted.

Using this analysis, it was found that the means of most prominent peaks for each dataset organized by weight and frequency averaged across participants are not

significantly different between both groups (Figure 25) (Wilkcoxon rank sum test, $p<0.05$).

For this conclusion, we carried an extensive analysis for all channels with visual event related responses, including Occipital, Occipital Parietal and Occipital Temporal regions (Figure 23).

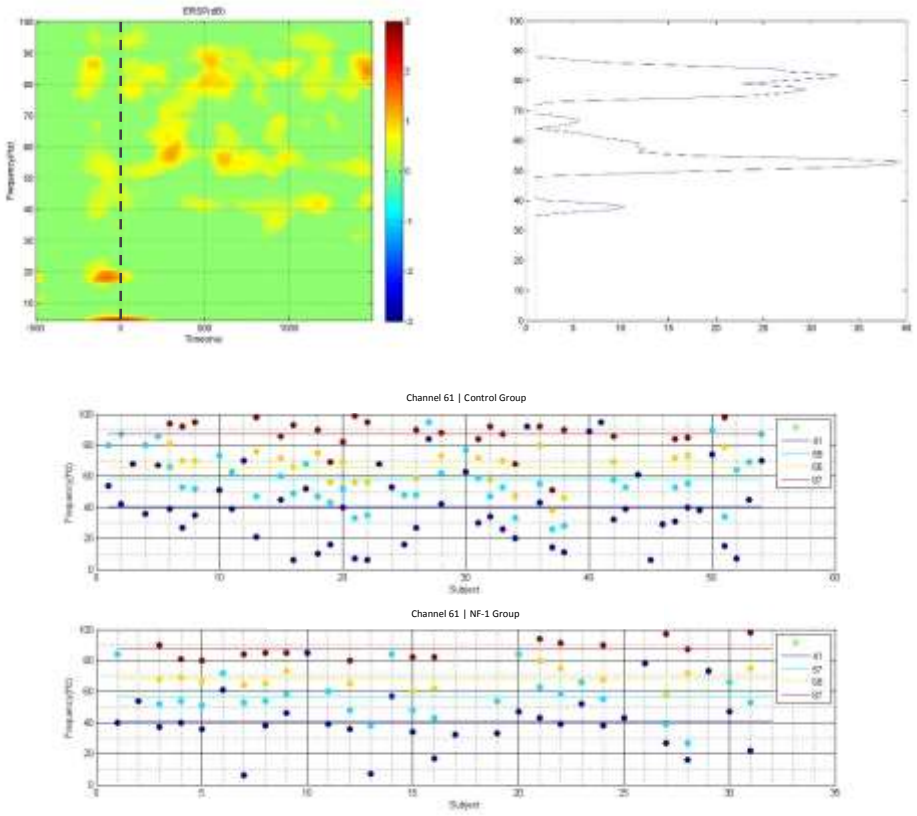


*Figure 25 – A) ERSP image and correspondent power mean (dB). B) Two outstanding peaks are visible (above 50Hz and above 80Hz). C) Scatter showing distribution of peaks found for each group and mean values for each frequency band (in Hz).*

Each frequency peak was labeled with one color (corresponding to the ascending order (in Hz) of all peaks found) up to a maximum of 4 peaks. The average was computed based in the frequency peaks found for each group and by color. For example, if subject A of control group has only two frequency peaks (*blue* and *cyan*), only those frequencies will enter for the averaging of all *blue* and *cyan* frequency ranges and the other ranges will receive no contribution for average calculations..

### *GABA levels do not correlate with gamma frequency bands*

After having established an automatic method of identifying of gamma peaks we attempted to replicate the findings of *Muthukumaraswamy et al.* (2009) [49], who found a relation between GABA levels and the identified gamma bands, especially a band ranged between 40Hz and 66Hz (stable in participants across repeated recording sessions).

In the previously mentioned study, a positive correlation between GABA and gamma frequency bands was identified with significant correlations (R=0.68, P=0.02). However, recent papers have come to refute these findings [50]. Here, using blob detection (2.3.2), we tried to correlate the identified frequency peaks with GABA levels. We attempted to replicate *Muthukumaraswamy et al.* (2009) results, by using the same frequency peaks range (30Hz – 80Hz) of control group subjects. We used as well an identical electrode location, averaging data from 4 channels (Figure 26).

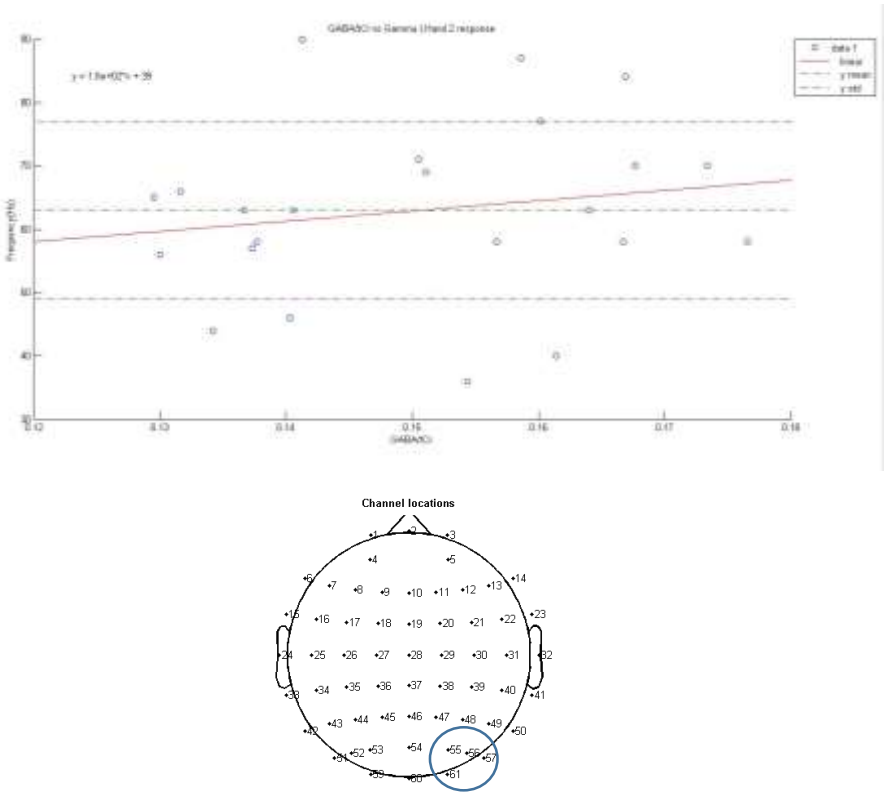


*Figure 26 - Control group relation between frequency peaks and GABA levels. No significant correlation was found between GABA concentration and peak of gamma frequency. In fact, the correlation coefficient obtained is so low(R<<0.1, p>0.5) as to make a positive linear correlation extremely unlikely.*

We extended the analysis, by applying a scanning window (Figure 27) algorithm to search for positive correlations among GABA levels and gamma peaks. The procedure started at 40Hz, with a 10Hz step (reaching 80Hz) and ±10Hz window. Gamma peaks found within the interval window were considered for the fitting. Missing values could exist, for example, when blob detection was not able to find gamma

The objective was to run all over the window, trying to find correlations in gamma, eventually in particular gamma sub-bands. Instead of the previous analysis (using a large window, 30Hz to 80Hz), we opted to evaluate data into smaller windows (20Hz width) trying to find putative correlations between sub-gamma bands and GABA levels. However, no significant correlations were found along all frequencies. Once again, only control subjects were evaluated here (correlation factor, R<<0.1). However, identical results were found for NF-1 Group (correlation factor, R<<0.1).

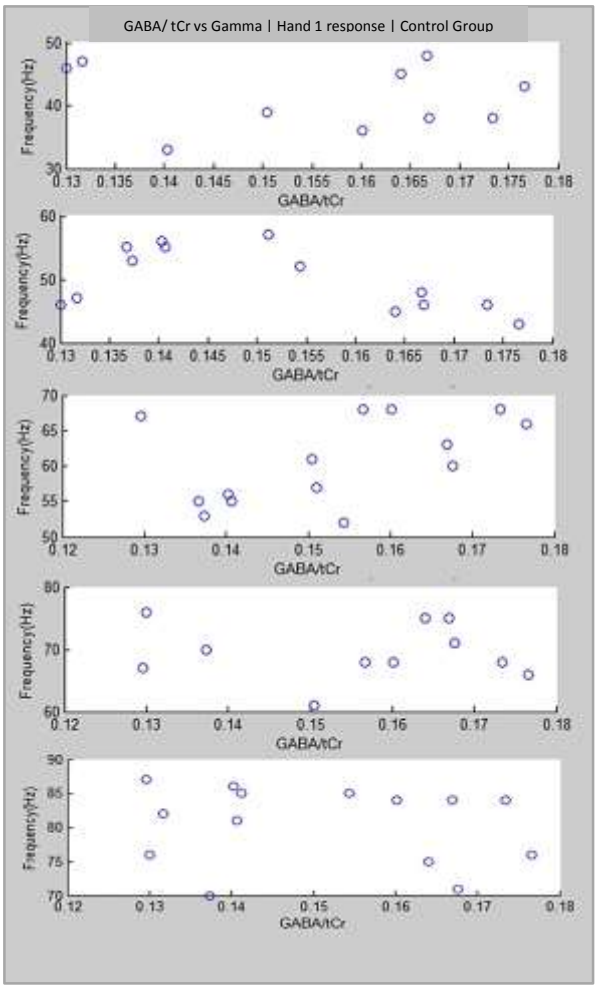


*Figure 27 – The "scanning window" algorithm append frequency in a window range of ±10Hz of a moving center starting at 40Hz, step of 10Hz and ending at 80 Hz. The image shows relations for one channel in Parietal Occipital cluster. Significant correlation coefficients were not found for any scatter graphs(R<<0.1, p>0.5).*

### *Glutamate/Glutamine (Glx) levels and BOLD hemodynamic levels do not correlate with gamma frequency bands*

For the evaluation of Glx levels and BOLD signals, the same protocol for GABA evaluation was performed, using identical window range (30Hz-80Hz) and blob detection.

Previously cited works[49,50] found no significant correlation between Glx and gamma peaks. Here, evaluating the Figure 26 cluster, no correlation was found, corroborating published analyses. The same was found for BOLD signals, where no significant relations were found. Once again, we represented frequencies in a window starting at 30 Hz, scattering each frequency peak with respective Glx or BOLD level. Obtained regressions have not significant correlation with data. No significant correlations were found when the window was divided on sub windows (equivalent evaluation to the Figure 27).

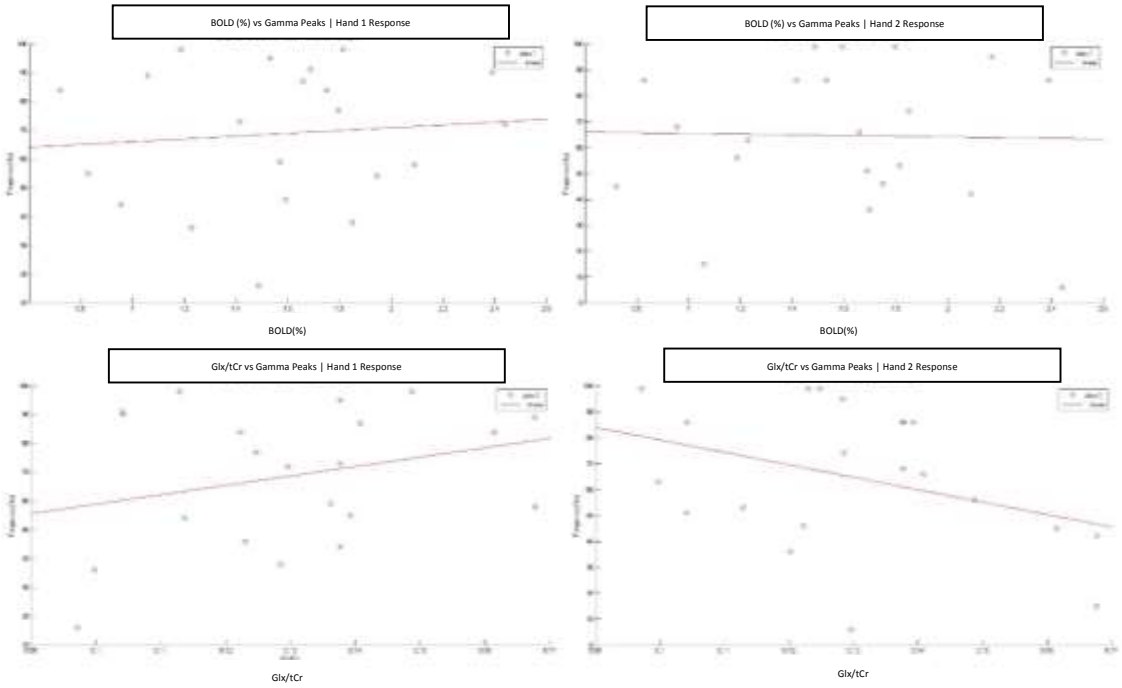


*Figure 28 – Bold and Glx/tCr relations with gamma peaks of control group on channel 57 (on the Occipital-Temporal cluster). Regressions models did not reach significance (R<<0.1, p>0.6).*

## 3.3 ERPCOH results

*NF-1 subjects show a distinct modulation of evoked phase coherence in the alpha band.*

The findings on ERSP analysis reveal nonexistence of significant differences between control and NF-1 subjects. Here, we will compare phase coherence results, in attempt to provide an association between known NF-1 deficits (like visuospatial or memory deficits[51]) and inter-hemispheric cluster phase coherence.

In a way to reduce computational time, we focused on visual brain areas for this analysis, since we are studying a visual stimulus, the main processing areas are the posterior ones. Thus, channel processing was performed starting at channel 33. Phase cross-coherence was computed between pairs of electrodes for each subject, for both groups. For greater statistical power, the data was analyzed for clusters, according to anatomical and functional properties of the underlying brain areas (Figure 29).

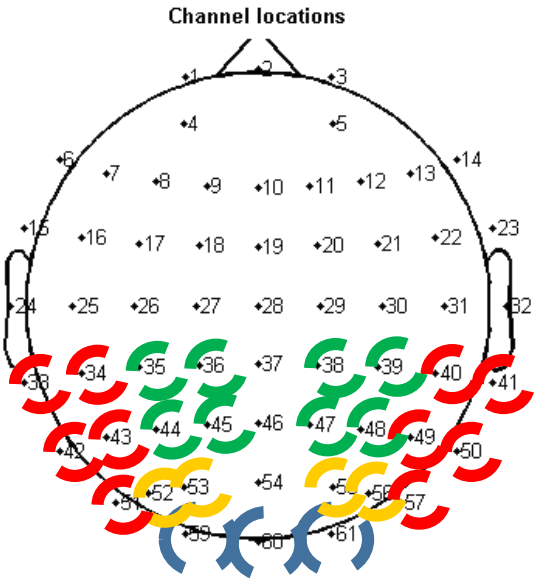


*Figure 29 - Distribution of channels according to 10-20 International system for a 64 channel cap. In red, Occipital Temporal cluster. In green, Parietal cluster. In yellow and blue, Parietal Occipital cluster and Occipital cluster, respectively.*

As a result of grand averaging analysis over all subjects, significant differences were found between groups, namely in the alpha band. A substantial decrease of alpha wave synchronization in NF-1 subjects was found compared with control group. This clear band, around 10Hz frequency (alpha band), started at 250 milliseconds and showed pronounced synchronization beyond 1500 milliseconds after the start of the

stimulus (Figure 30, 31). This result is unexpected, because it was not previously documented in this NF-1 disorder

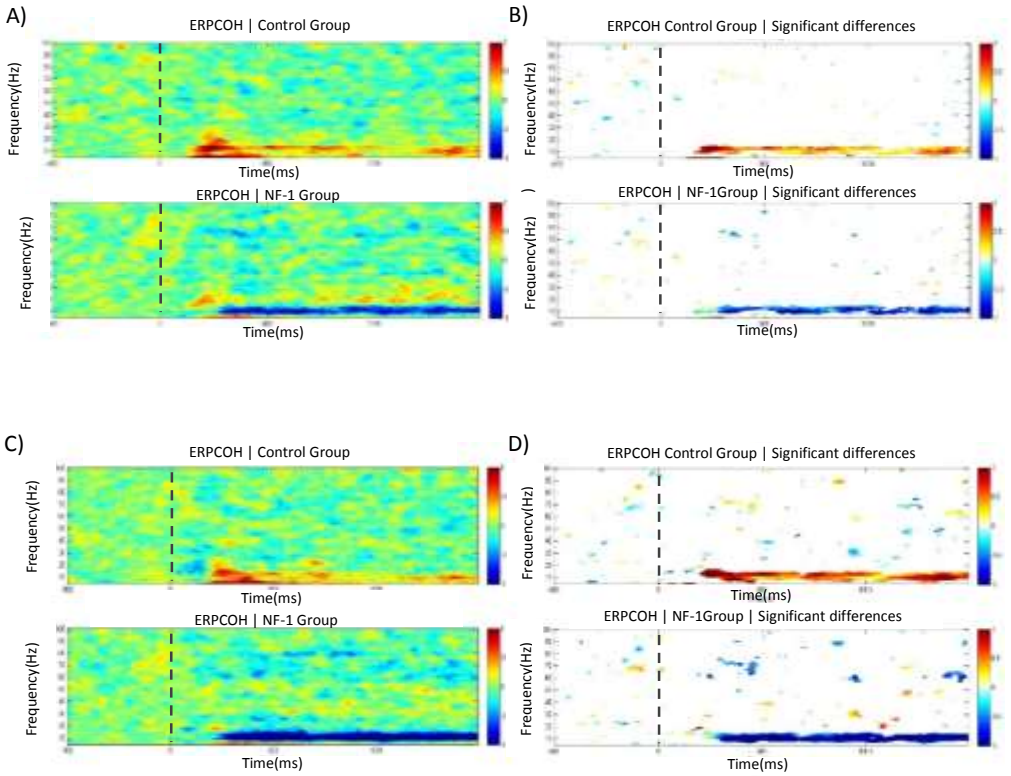


*Figure 30 - A, C) Comparison between phase-coherence between Occipital cluster and left Occipital Parietal cluster, respectively. In B, D) Significant data between groups (respectively to left image), after Wilkcoxon rank-sum tests (p<0.0001). Alpha band start at approximately 250 milliseconds after stimulus start and remain constant beyond 1500 milliseconds.*

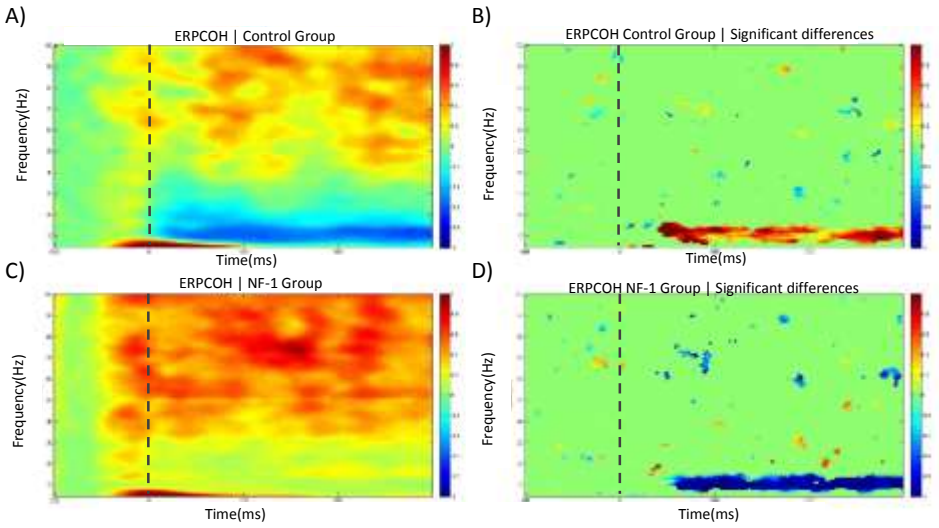


*Figure 31 - A, C).ERSP averages for Occipital Parietal cluster (right and left sides) In B, D) Comparison between phase-coherence between Occipital cluster and left Occipital Parietal cluster, respectively. Significant data between groups (respectively to left image), after Wilkcoxon rank-sum tests (p<0.0001). The alpha band starts at approximately 250 milliseconds after stimulus start and remains constant beyond 1500 milliseconds.*

Furthermore, the power alpha waves is reduced in the control group after the stimulus onset, when compared with NF-1 group. This provides relevant information, because it makes unlikely that the increased phase coherence is a result of volume conduction, reinforcing the statistical power of the results.

# 4 Discussion

## 4.1 The methodological processes

### 4.1.1 The analysis context

In the field of EEG analysis, there are different approaches, like the way that information is acquired, processed and displayed or also which are the different processing methods and what information that can be extracted from them. It is imperative to know the rationale behind these techniques, their strengths and weaknesses. Given the nature of EEG signals, it is possible to analyze neural processes at a better time resolution than other brain functional acquisition techniques.

However, even decades after the first steps in EEG, there is still no appropriately standardized evaluation of data in most of the cases. For this reason, the clinical use of EEG is still limited. The existence of biased evaluations of EEG data can result in situations where different conclusions, even contradicting ones, can be drawn about the same paradigm, mudding the conclusions taken when studying brain activity using this technique.

### 4.1.2 The Methodological approaches

In a way to avoid these subjective evaluations, my first purpose was to construct an unbiased method of analysis for time-frequency images, applied particularly to ERSP spectra, in this work. This method includes automated pre-processing which, by itself, is a helpful way to reduce time with laborious manual pre-processing and also offers a way of further standardizing the analysis.

The main process of automatically finding frequency bands of interest was chosen in a paradigm where there is no concise premises of “what” a band is and “where” it should be found (i.e. which and how many frequencies it encompasses, at what time it starts and stops). This detail makes things particularly harder to explore. There is no clear way to define a band on ERSP images so the first step was to explore ways of narrowing the requisites a band of evoked activity should have to make its physiological significance likely.

The first methodological approach, i.e. finding the four main peaks in each of the pre-established classical frequency bands, attempted to unravel the concept of band and which are the parameters in ERSP spectrum that can define it. The averaged ERSP’s

along frequencies (Figure 25) is a good start pointing when searching for bands. However, oscillatory characteristics of neural mechanisms involve ERS's and ERD´s, most of times in the same frequency band, a factor that will dilute averages. The consequence is that Gaussian distribution peaks may not involve the existence of an identifiable band.

Furthermore, the method is not completely data-driven, because some parameters have pre-defined characteristics (for example, the number of maximum peaks that algorithm is able to find for compute averages for the bands, Figure 18)

The second methodological approach focuses on solving and parameterizing the concept of "band". Applying the threshold value (variable according to bootstrapping information, in dB), regions of interest are shown, the so called blobs. These blobs are relevant information and, operating with the right restrictions, they can be a powerful tool to localize frequency bands that may potentially play a role in neurophysiology and in cognitive functions.

### 4.1.3 Limitations of the methodological approaches.

The best approximation to a standardized methodological process capable of identifying bands on time-frequency plots is the second methodological approach, not only because of its flexibility in terms of adding add new features to algorithm, increasing its strength, but also because it is an almost fully data-driven method.

The identification of blobs, according to the previously established parameters, appears to be an adequate approximation of ERSs encompassing several frequency bands. Nevertheless, some limitations persist. In some cases, thresholds are not suited for the adequate isolation of blobs. For example: a too low threshold applied to ERSP spectra will isolate blobs extending for too many frequencies in the frequency axis (i.e. "thick" bands in the spectrum), occupying sometimes more than 30Hz extension, and automatic evaluation is not prepared to reject this type of information. In an ideal situation, threshold values should automatically increase, creating smaller blobs, allowing for their right identification. Validation is also clearly a sensitive point, due to the ambiguous character of bands. The bands identified by experienced researchers are not always the same bands, as expected, which creates a substantial problem when looking for a validating process.

At the moment, the methodological approach is suitable, but future improvements are still necessary to increase its robustness.

## 4.2 Relationship between ERSPs, GABA and BOLD signal

Recently reported findings about the correlation between gamma band frequencies (30Hz-80Hz) and other physiological parameters might not hold as previous thought. About task related signals, well defined but subject specific gamma band activity is difficult to determine. Moreover, the alleged relationship between hemodynamic signals and gamma band activity may not be as linear as expected. In fact, using a relatively unbiased method based on well-grounded assumptions regarding the expected "shape" of a gamma band with underlying activity related to a visual task, this purported relation was not found. However, some considerations must be taken in account, there is no way to definitely prove that this relation does not exist[23,24,52].

BOLD signal and GABA levels have been reported as related mechanisms that relate to the balance excitation-inhibition which sets the peak of gamma oscillations on a given neural network (composed by pyramidal cells and GABAergic inhibitory interneurons[5,53,54]). We were able to search for such correlations using data acquired with magnetic resonance spectroscopy (procedures and methods described in *Inês R. Violante et al.*(2014)).

The BOLD signal is dependent on brain activity and therefore with gamma oscillations. GABA concentration measured with MRS indicates the bulk concentration in a large voxel and not the activity of the interneurons in that region.

Effectively, GABA concentrations and BOLD values (relative percentage) accuracy measures can be high, however, when related with EEG signals, spatial accuracy may be lost. While GABA and BOLD values are measured at the level of voxels in a limited region of the occipital cortex, ERSP represents activity from one or several unknown sources recorded from the surface by electrodes which offer a much worse spatial resolution given the effects of volume conduction and fading of the electrical signal (mainly due to volume conduction of EEG signal). This point can be critical, in a way that spatial accuracy is compromised.

Relating this matter with previous considerations (4.1.2) about methodological approaches to identify gamma bands, possibly we are creating a model that cannot take into account all variables, introducing uncertainty. We might not have sufficient information for full characterization and classification of physiological phenomena of oscillatory patterning, due to the large range of related parameters, for example, the related sources of oscillations or associated genetics.

To increase the viability of the processing approaches, adjustments and more information have to be contemplated, namely using ICA and sourcing tools. ICA, for example, may enable the possibility to separate different acquired sources for a determined channel. Sources will normally contain information from more specific spatial locations.

## 4.3 Phase coherence considerations

Neurofibromatosis type-1 is a neurodevelopmental disorder, with major prevalence deficits on visual perception, motor, language, memory and attention domains[51]. Some advances show, for example, that NF-1 individuals have increased lapses of attention and visual sensitivity deficits, as a result of abnormal later stages of visual processing and enhanced amplitude of alpha waves[16].

Although in this work no significant amplitude differences were found, at least for the stimulus evoked ones, the phase synchrony results seems to be remarkable. The pronounced differences in phase synchrony in alpha bands between clusters (especially inter-hemispheric) can help to explain deficits on visual processing information and attention deficits. Actually, there are no previously published findings on the significant differences on phase synchrony on NF-1 individuals, especially on alpha band.

Alpha band has been related as relevant to cognitive functions, such as attention, consciousness, visuospatial and long range synchronization[2,11,55,18]. These findings suggests the existence of a link between any NF-1 deficit individuals and any of these functions that alpha bands are evolved. The changes in alpha phase synchrony offer a promising avenue of research for the study of NF-1 related deficits.

Furthermore, an exhaustive coherence evaluation can be performed for all scalp recorded channels and be related to particular NF-1 deficits, namely attention lapses.

## 4.4 Conclusion

The theoretical component in this work allowed to enlarge my knowledge with especially related with EEG technique and its processing demands and helped to understand a way to analyze the relation of these signals with cognitive mechanisms with an especial relevance on visual perception

The developed work with real clinical neuroscience data, in a controversial area where analyses approaches are not yet standardized was a rewarding one. In this context, an extensive work pipeline was carried out, in a way that some progress, namely in the implementation of pre-processing routines and alternative methodological approaches, was achieved, simplifying data processing, especially for large amounts of data. This represents a first step for an unbiased analysis of time-frequency information of brain oscillations, as well as phase coherence.

Furthermore, an important result arised from the analyzed data, allowing to understand patterns of changes in NF-1, particularly with regard to the analysis of the phase coherence, which may represent an useful biomarker.

In sum, this thesis does not answer all technical and scientific questions, but hopefully provides a step forward in the process of classification of oscillatory patterns in a standardized and automated manner.

# 5 Bibliography

1. Brodal, P. *The central nervous system: Structure and function*. *Arch. Neurol.* (2004). at <http://scholar.google.com/scholar?hl=en&btnG=Search&q=intitle:No+Title#0>

2. Uhlhaas, P. J., Haenschel, C., Nikolić, D. & Singer, W. The role of oscillations and synchrony in cortical networks and their putative relevance for the pathophysiology of schizophrenia. *Schizophr. Bull.* **34,** 927–43 (2008).

3. Uhlhaas, P. J. Dysconnectivity, large-scale networks and neuronal dynamics in schizophrenia. *Curr. Opin. Neurobiol.* **23,** 283–90 (2013).

4. Olejniczak, P. Neurophysiologic basis of EEG. *J. Clin. Neurophysiol.* **23,** 186–9 (2006).

5. Logothetis, N. K. What we can do and what we cannot do with fMRI. *Nature* **453,** 869–78 (2008).

6. Elston, G. N. Cortex, Cognition and the Cell: New Insights into the Pyramidal Neuron and Prefrontal Function. *Cereb. Cortex* **13,** 1124–1138 (2003).

7. Sanei, S. & Chambers, J. *EEG signal processing*. (2008). at <http://books.google.com/books?hl=en&lr=&id=vIuCV2IKwasC&oi=fnd&pg=PR5&dq=EEG+Signal+Processing&ots=vhzj4fE_mF&sig=T8MR9IVQcwWAXPdHJDAGqAel4ug>

8. Lachaux, J. P., Rodriguez, E., Martinerie, J. & Varela, F. J. Measuring phase synchrony in brain signals. *Hum. Brain Mapp.* **8,** 194–208 (1999).

9. Buzsaki, G. *Rhythms of the Brain*. (Oxford University Press, 2006). doi:10.1093/acprof:oso/9780195301069.001.0001

10. Wang, X. Rhythms in Cognition. **90,** 1195–1268 (2010).

11. Başar, E., Başar-Eroglu, C., Karakaş, S. & Schürmann, M. Gamma, alpha, delta, and theta oscillations govern cognitive processes. *Int. J. Psychophysiol.* **39,** 241–8 (2001).

12. Başar, E., Başar-Eroğlu, C., Karakaş, S. & Schürmann, M. Brain oscillations in perception and memory. *Int. J. Psychophysiol.* **35,** 95–124 (2000).

13. Sutter, R. & Kaplan, P. W. Electroencephalographic Patterns in Coma : When Things Slow Down. 201–209 (2012).

14. Jones, M. W. & Wilson, M. a. Theta rhythms coordinate hippocampal-prefrontal interactions in a spatial memory task. *PLoS Biol.* **3,** e402 (2005).

15. Melloni, L. *et al.* Synchronization of neural activity across cortical areas correlates with conscious perception. *J. Neurosci.* **27,** 2858–65 (2007).

16. Ribeiro, M. J. *et al.* Abnormal late visual responses and alpha oscillations in neurofibromatosis type 1: a link to visual and attention deficits. *J. Neurodev. Disord.* **6,** 4 (2014).

17. Hanslmayr, S. *et al.* Visual discrimination performance is related to decreased alpha amplitude but increased phase locking. *Neurosci. Lett.* **375,** 64–8 (2005).

18. Klimesch, W. A-Band Oscillations, Attention, and Controlled Access To Stored Information. *Trends Cogn. Sci.* **16,** 606–17 (2012).

19. Melani, F., Zelmann, R., Mari, F. & Gotman, J. Continuous High Frequency Activity: a peculiar SEEG pattern related to specific brain regions. *Clin. Neurophysiol.* **124,** 1507–16 (2013).

20. Pires, G., Nunes, U. & Castelo-Branco, M. Comparison of a row-column speller vs. a novel lateral single-character speller: assessment of BCI for severe motor disabled patients. *Clin. Neurophysiol.* **123,** 1168–81 (2012).

21. Deiber, M.-P., Ibañez, V., Missonnier, P., Rodriguez, C. & Giannakopoulos, P. Age-associated modulations of cerebral oscillatory patterns related to attention control. *Neuroimage* **82,** 531–46 (2013).

22. Rangaswamy, M. *et al.* Beta power in the EEG of alcoholics. *Biol. Psychiatry* **52,** 831–42 (2002).

23. Neuenschwander, S., Castelo-Branco, M. & Singer, W. Synchronous oscillations in the cat retina. *Vision Res.* **39,** 2485–97 (1999).

24. Niessing, J. *et al.* Hemodynamic signals correlate tightly with synchronized gamma oscillations. *Science* **309,** 948–51 (2005).

25. Castelhano, J., Rebola, J., Leitão, B., Rodriguez, E. & Castelo-Branco, M. To perceive or not perceive: the role of gamma-band activity in signaling object percepts. *PLoS One* **8,** e66363 (2013).

26. Tallon-Baudry, C., Bertrand, O., Delpuech, C. & Pernier, J. Stimulus specificity of phase-locked and non-phase-locked 40 Hz visual responses in human. *J. Neurosci.* **16,** 4240–9 (1996).

27. Malsburg, C. Von Der. The What and Why of Binding : The Modeler ' s Perspective. **24,** 95–104 (1999).

28. Herrmann, C. S., Munk, M. H. J. & Engel, A. K. Cognitive functions of gamma-band activity: memory match and utilization. *Trends Cogn. Sci.* **8,** 347–55 (2004).

29. Gray, C. M. The temporal correlation of Visual Feature Integration: Still Alive and Well. **24,** 31–47 (1999).

30. Velik, R. From simple receptors to complex multimodal percepts: a first global picture on the mechanisms involved in perceptual binding. *Front. Psychol.* **3,** 259 (2012).

31. Castelhano, J. & Castelo-Branco, M. Neural substrates of 2D/3D object perception: a combined EEG/fMRI approach. (2014). doi:ISBN: 978-989-20-4919-9

32. Buzsáki, G. & Wang, X.-J. Mechanisms of gamma oscillations. *Annu. Rev. Neurosci.* **35,** 203–25 (2012).

33. Tzelepi, a, Bezerianos, T. & Bodis-Wollner, I. Functional properties of sub-bands of oscillatory brain waves to pattern visual stimulation in man. *Clin. Neurophysiol.* **111,** 259–69 (2000).

34. Tallon-baudry, C. The roles of gamma-band oscillatory synchrony in human visual cognition. 321–332 (2009).

35. Gaona, C. M. *et al.* Nonuniform high-gamma (60-500 Hz) power changes dissociate cognitive task and anatomy in human cortex. *J. Neurosci.* **31,** 2091–100 (2011).

36. Donald L. Schomer MA, MD, Fernando H. Lopes da Silva MD, P. Niedermeyer's-Electroencephalography-Basic-Principles,-Clinical-Applications,-and-Related-Fields,-6th-Edition.

37. Muthukumaraswamy, S. D., Singh, K. D., Swettenham, J. B. & Jones, D. K. Visual gamma oscillations and evoked responses: variability, repeatability and structural MRI correlates. *Neuroimage* **49,** 3349–57 (2010).

38. Makeig, S. Auditory event-related dynamics of the EEG spectrum and effects of exposure to tones. *Electroencephalogr. Clin. Neurophysiol.* **86,** 283–93 (1993).

39. Engel, a K., Fries, P. & Singer, W. Dynamic predictions: oscillations and synchrony in top-down processing. *Nat. Rev. Neurosci.* **2,** 704–16 (2001).

40. Luck, S. J. *An Introduction to the Event-Related Potential Technique*. 388 (2005).

41. Reviewed, P. Previously Published Works. (2004).

42. Roach, B. J. & Mathalon, D. H. Event-related EEG time-frequency analysis: an overview of measures and an analysis of early gamma band phase locking in schizophrenia. *Schizophr. Bull.* **34,** 907–26 (2008).

43. Delorme, A. & Makeig, S. EEGLAB: an open source toolbox for analysis of single-trial EEG dynamics including independent component analysis. *J. Neurosci. Methods* (2004). at <http://www.sciencedirect.com/science/article/pii/S0165027003003479>

44. Violante, I. R. *et al.* GABA deficit in the visual cortex of patients with neurofibromatosis type 1: genotype-phenotype correlations and functional impact. *Brain* **136,** 918–25 (2013).

45. Başar, E. & Güntekin, B. A review of brain oscillations in cognitive disorders and the role of neurotransmitters. *Brain Res.* **1235,** 172–93 (2008).

46. Pires, G., Castelo-Branco, M. & Nunes, U. Visual P300-based BCI to steer a wheelchair: a Bayesian approach. *Conf. Proc. IEEE Eng. Med. Biol. Soc.* **2008,** 658–61 (2008).

47. Pires, G., Nunes, U. & Castelo-Branco, M. GIBS block speller: toward a gaze-independent P300-based BCI. *Conf. Proc. IEEE Eng. Med. Biol. Soc.* **2011,** 6360–4 (2011).

48. Bernardino, I., Castelhano, J., Farivar, R., Silva, E. D. & Castelo-Branco, M. Neural correlates of visual integration in Williams syndrome: gamma oscillation patterns in a model of impaired coherence. *Neuropsychologia* **51,** 1287–95 (2013).

49. Muthukumaraswamy, S. D., Edden, R. a E., Jones, D. K., Swettenham, J. B. & Singh, K. D. Resting GABA concentration predicts peak gamma frequency and fMRI amplitude in response to visual stimulation in humans. *Proc. Natl. Acad. Sci. U. S. A.* **106,** 8356–61 (2009).

50. Cousijn, H. *et al.* Resting GABA and glutamate concentrations do not predict visual gamma frequency or amplitude. *Proc. Natl. Acad. Sci. U. S. A.* **111,** 9301–6 (2014).

51. Violante, I. R. *et al.* Abnormal brain activation in neurofibromatosis type 1: a link between visual processing and the default mode network. *PLoS One* **7,** e38785 (2012).

52. Castelo-Branco, M., Neuenschwander, S. & Singer, W. Synchronization of visual responses between the cortex, lateral geniculate nucleus, and retina in the anesthetized cat. *J. Neurosci.* **18,** 6395–410 (1998).

53. Bartos, M., Vida, I. & Jonas, P. Synaptic mechanisms of synchronized gamma oscillations in inhibitory interneuron networks. *Nat. Rev. Neurosci.* **8,** 45–56 (2007).

54. Mazzoni, A., Panzeri, S., Logothetis, N. K. & Brunel, N. Encoding of naturalistic stimuli by local field potential spectra in networks of excitatory and inhibitory neurons. *PLoS Comput. Biol.* **4,** e1000239 (2008).

55. Doesburg, S. M., Green, J. J., McDonald, J. J. & Ward, L. M. From local inhibition to long-range integration: a functional dissociation of alpha-band

synchronization across cortical scales in visuospatial attention. *Brain Res.* **1303,** 97–110 (2009).